

## The geological history of the Latimojong region of western Sulawesi

Lloyd T. White<sup>1∞\*</sup>, Robert Hall<sup>1</sup>, Richard A. Armstrong<sup>2</sup>, Anthony J. Barber<sup>1</sup>,  
Marcelle BouDagher Fadel<sup>3</sup>, Alan Baxter<sup>4,5</sup>, Koji Wakita<sup>6</sup>, Christina Manning<sup>7</sup>, Joko  
Soesilo<sup>8</sup>

1. Southeast Asia Research Group, Department of Earth Sciences, Royal Holloway University of London, Egham, Surrey, TW20 0EX
2. Research School of Earth Sciences, The Australian National University, Canberra, Australia, 0200
3. Department of Earth Sciences, University College London, Gower Street, London, WC1E 6BT, UK
4. School of Environmental and Rural Sciences, University of New England, Armidale, New South Wales, Australia, 2351
5. Department of Earth and Planetary Sciences, McGill University, Montreal, Canada
6. Department of Earth Sciences, Yamaguchi University, Yamaguchi, Japan
7. Department of Earth Sciences, Royal Holloway University of London, Egham, Surrey, TW20 0EX
8. Faculty of Mineral Technology, UPN Veteran Yogyakarta, Jalan SWK104, 52283, Yogyakarta, Indonesia

\* Corresponding Author

∞ Present address: School of Earth and Environmental Sciences, University of Wollongong, Northfields Avenue, Wollongong, NSW, Australia, 2522

### Research Highlights

- We review the stratigraphy and tectonic history of the Latimojong Mountains region.
- We found that the Latimojong Formation does not occur in this region.
- We present new fossil ages for the Toraja Fm., Makale Fm. And Enrekang Volcanics
- We present new U-Pb zircon SHRIMP data for igneous rocks in the region.
- The region is dominated by strike-slip faulting.

34 **Abstract**

35 We present an updated geological map and revised stratigraphy of the Latimojong  
36 region of central–western Sulawesi. This work includes new biostratigraphic ages  
37 from the Latimojong Metamorphic Complex, Toraja Group, Makale Formation and  
38 Enrekang Volcanics, together with whole-rock geochemical data and sensitive high-  
39 resolution ion microprobe (SHRIMP) U-Pb analyses from zircons extracted from  
40 igneous rocks in the region. Previous work on the study region and in other parts of  
41 Sulawesi have discussed the age and character of two different rock sequences with  
42 similar names, the Latimojong Complex and the Latimojong Formation. One would  
43 assume that the type location for these two sequences is in the Latimojong Mountains.  
44 However, there is considerable confusion as to the character and location of these  
45 sequences. We make a distinction between the Latimojong Formation and the  
46 Latimojong Complex, and propose that the Latimojong Complex be renamed the  
47 *Latimojong Metamorphic Complex* to minimise the confusion associated with the  
48 current nomenclature. The Latimojong Metamorphic Complex is an accretionary  
49 complex of low- to high-grade metamorphic rocks tectonically mixed with cherts and  
50 ophiolitic rocks, while the Latimojong Formation consists of Upper Cretaceous  
51 weakly deformed, unmetamorphosed sediments or very low-grade metasediments  
52 (previously interpreted as flysch or distal turbidites that unconformably overlie older  
53 rocks). Our work indicates that the Latimojong Formation must be restricted to  
54 isolated, unobserved segments of the Latimojong Mountains, or are otherwise not  
55 present in the Latimojong region, meaning the Latimojong Formation would only be  
56 found further north in western Sulawesi. Radiolaria extracted from chert samples  
57 indicate that the Latimojong Metamorphic Complex was likely assembled during the  
58 Cretaceous (Aptian-Albian) and was later metamorphosed. Ages obtained from  
59 benthic and planktonic foraminifera were used to differentiate and map the Toraja  
60 Group (Ypresian to Chattian: 56–23 Ma), Makale Formation (Burdigalian to  
61 Serravallian: 20.5–11.5 Ma) and Enrekang Volcanic Series (8.0–3.6 Ma) across the  
62 study area. U-Pb isotopic data collected from magmatic zircons record several phases  
63 of volcanism (~38 Ma, ~25 Ma and 8.0–3.6 Ma) in the region. Each phase of  
64 magmatism can be distinguished according to petrology and whole-rock geochemical  
65 data. The isotopic ages also show that dacites from the Enrekang Volcanic Series are  
66 contemporaneous with the emplacement of the Palopo Granite (6.6–4.9 Ma). Miocene  
67 to Proterozoic inherited zircons within these igneous rocks support earlier suggestions

68 that Sulawesi potentially has a Proterozoic–Phanerozoic basement or includes  
69 sedimentary rocks (and therefore detrital zircons) derived from the erosion of  
70 Proterozoic or younger material. Some earlier work proposed that the granitic rocks in  
71 the region developed due to crustal melting associated with plate collision and  
72 radiogenic heating. Our observations however, support different interpretations,  
73 where the granites are associated with arc magmatism and/or crustal extension. The  
74 region was cross-cut by major strike-slip fault zones during the Pliocene. This  
75 deformation and the buoyancy associated with relatively young intrusions may have  
76 facilitated uplift of the mountains.

77

## 78 **1. Introduction**

79 The study area, herein referred to as the Latimojong region, comprises the Latimojong  
80 Mountains of central-west Sulawesi and the surrounding areas, including Tanah  
81 Toraja to the west (Fig. 1 and 2). This mountainous area includes the highest peaks  
82 found on Sulawesi, with some exceeding 3,400 m a.s.l (e.g. Rante Mario). The region  
83 is considered to include part of a Cretaceous accretionary complex and records several  
84 phases of deformation potentially associated with continent collision (Bergman et al.,  
85 1996). Existing geological maps of the region vary in quality and there is poor age  
86 control for many of the sequences in the area. We present the results of a geological  
87 study of the Latimojong Mountains. This included the collection of new age,  
88 geochemical and structural information to re-evaluate existing geological maps as  
89 well as the stratigraphy and deformation history of the region.

90

## 91 **2. The geological framework of Sulawesi**

92 Sulawesi is a region of amalgamated continental blocks and island arc crust that  
93 records a Cretaceous to recent history of continent-continent collision, ophiolite  
94 obduction, arc volcanism, strike-slip faulting and significant crustal extension (e.g.  
95 Katili, 1970, 1978; Audley-Charles, 1974; Hamilton, 1979; Parkinson, 1998; Spencer,  
96 2010, 2011; Hennig et al., 2016; van Leeuwen et al., 2016). These processes are  
97 recorded in different parts of the island and this resulted in a complex geology, as is  
98 shown in Figure 1. To provide further context, there was collision between different  
99 parts of Sulawesi causing ophiolite emplacement (e.g. Audley-Charles, 1974;  
100 Hamilton, 1979; Sukanto and Simandjuntak, 1983; Coffield et al., 1993; Bergman et  
101 al., 1996; Parkinson, 1998). This is interpreted to represent an arc-continent collision

102 between the micro-continental Sula Spur and North Arm of Sulawesi in the Early  
103 Miocene (e.g. Audley-Charles, 1974; Hamilton, 1979; Sukanto and Simandjuntak,  
104 1983; Coffield et al., 1993; Bergman et al., 1996; Hall, 1996; 2002, 2012; van  
105 Leeuwen and Muhardjo, 2005; van Leeuwen et al., 2007; Spakman and Hall 2010;  
106 Watkinson et al. 2011). This period of collision was followed or accompanied by  
107 Middle Miocene to Pliocene phases of magmatism and metamorphism in western and  
108 north Sulawesi (e.g. Bergman et al., 1996; Elburg and Foden, 1999a; 1999b; Elburg et  
109 al., 2003; van Leeuwen et al., 2007; 2016; Spencer, 2010; 2011; Hennig et al., 2016)  
110 and strike-slip faulting (Katili, 1970; 1978; Hamilton, 1979; van Leeuwen, 1981;  
111 Sukanto, 1982; Silver et al., 1983a; 1983b; Berry and Grady, 1987; Simandjuntak et  
112 al., 1994; Surono, 1994; Jaya and Nishikawa, 2013; White et al., 2014; Hennig et al.,  
113 2016; van Leeuwen et al., 2016). The uplift associated with collision, together with  
114 other episodes of deformation and uplift, led to the exhumation of several  
115 metamorphic basement inliers. This includes the Cretaceous Baru and Bantimala  
116 complexes in south-western Sulawesi, as well as similar rocks in the Latimojong  
117 Mountains, ~100-150 km to the NNE (e.g. Coffield et al., 1993; Bergman et al., 1996;  
118 Wakita et al., 1996; Parkinson et al., 1998). These basement rocks are unconformably  
119 overlain by Upper Cretaceous turbidite deposits (e.g. the Balangbaru and Marada  
120 formations) and have been cross-cut by numerous faults (e.g. Querubin and Walters,  
121 2012).

122

### 123 **3. The Geology of the Latimojong region**

124 The Latimojong region is located to the west and southwest of Palopo, a town on the  
125 northwestern coast of Bone Bay (Fig. 2). It is quite rugged, mountainous and heavily  
126 forested terrane, and therefore the fieldwork that has been conducted in this region to  
127 date has largely been restricted to an E-W section across the western slope of the  
128 mountain range and along parts of the eastern margin of the mountain range. The  
129 geology of the area, very simply, consists of a mountainous inlier of metasediments as  
130 well as gabbro, basalt and serpentinite, as well as several carbonate sequences and  
131 various Mio-Pliocene intrusions and volcanics (Fig. 2).

132

133 The first reports on the study area were provided by Dutch geologists before World  
134 War II (e.g. Brouwer, 1934). Geologists from the Geological Research and  
135 Development Centre (GRDC) later mapped this region and other parts of Sulawesi at

136 1:250,000 scale during the 1970's and 1980's (e.g. Djuri and Sudjarmiko, 1974;  
137 Simandjuntak et al., 1991). Isotopic dating and geochemical studies have provided  
138 information on the age and nature of igneous rocks in the region (e.g. Priadi et al.,  
139 1994; Bergman et al., 1996; Polvé et al., 1997; Elburg et al., 2003; Elburg and Foden,  
140 1998; 1999a; 1999b) and there have been continued efforts to document the  
141 stratigraphic and structural history (Coffield et al., 1993; Bergman et al., 1996;  
142 Baharuddin and Harahap, 2000; Endaharto, 2000). Several reports also discuss the  
143 local geology of the Awak Mas orogenic gold deposit that is found in the Latimojong  
144 Mountains (e.g. van Leeuwen and Pieters 2011; Querubin and Walters 2012).

145

146 Despite this earlier work, there is still considerable uncertainty about the region's  
147 stratigraphy, structural architecture and deformation history. Current understanding of  
148 the stratigraphy is based on 1:250,000 mapping and aerial photographic interpretation  
149 as well as sparse biostratigraphic data (e.g. Djuri and Sudjarmiko, 1974; Coffield et  
150 al., 1993; Bergman et al., 1996). Furthermore, conflicting radiometric age data have  
151 been reported based on different isotopic systems used to date the same rocks (e.g.  
152 low temperature thermochronology results are older than conventional ID-TIMS U-Pb  
153 crystallization ages of zircon reported by Bergman et al., 1996). Also, as relatively  
154 few studies have been conducted in the Latimojong region, much about its geology  
155 has been inferred from comparisons to similar sequences of rocks exposed in other  
156 parts of Sulawesi (e.g. Sukanto and Simandjuntak, 1983; van Leeuwen and  
157 Muhandjo, 2005; Calvert and Hall, 2007; Hennig et al., 2016). These comparisons  
158 with other areas have led to considerable confusion about the nomenclature that is  
159 used to define the stratigraphy of western Sulawesi. We therefore attempt to resolve  
160 these issues and report new biostratigraphic data from cherts and carbonate rocks as  
161 well as new U-Pb zircon ages for granitoids and volcanic rocks across the Latimojong  
162 region.

163

### 164 3.1 The Latimojong Complex and the Latimojong Formation

165 The oldest units exposed in the region are weakly to moderately metamorphosed  
166 rocks that include grey to black slates, phyllites, cherts, marbles, quartzites and  
167 silicified breccia that are intruded by intermediate to basic rocks (Djuri and  
168 Sudjarmiko, 1974; Coffield et al., 1993; Bergman et al., 1996; Djuri et al., 1998;  
169 Querubin and Walters 2012). Djuri and Sudjarmiko (1974) classified all of these rocks

170 as part of the “Latimojong Formation”. However, later workers subsequently used the  
171 same name to define a series of thinly bedded sandstone and laminated shale deposits  
172 or ‘flysch’ deposits found to the west, north-west and north of the Latimojong  
173 Mountains (Sukamto and Simandjuntak, 1983; Ratman and Atmawinata, 1993;  
174 Hadiwijoyo et al., 1993; Simandjuntak et al., 1991; van Leeuwen and Muhardjo,  
175 2005; Calvert and Hall, 2007; van Leeuwen et al., 2016; Hennig et al., 2016). These  
176 sandstones and shales are not metamorphosed or have a low-grade metamorphic  
177 character.

178

179 The most detailed descriptions of the “Latimojong Formation” are therefore from  
180 other areas, most of which are many tens to hundreds of kilometers from the  
181 Latimojong region. This includes the distal turbidite sequences from the Lariang  
182 region as described by Calvert (2000) and van Leeuwen and Muhardjo (2005).  
183 Calvert (2000) reported dark grey shales with varying amounts of siltstones and  
184 occasionally fine sandstone, with rare medium sandstone, locally with flute casts,  
185 while van Leeuwen and Muhardjo (2005) described these as weakly metamorphosed  
186 pelitic and fine-grained psammitic rocks. These sequences and their equivalents in the  
187 Karama area yield Coniacian-Maastrichtian ages from nannofossil and foraminifera  
188 (Chamberlain and Seago, 1995), Cretaceous detrital zircons (van Leeuwen and  
189 Muhardjo, 2005) and Cretaceous ammonites (Reijzer 1920). Cretaceous (Campanian  
190 to early Maastrichtian) ages were also reported for similar rocks from the Mamuju  
191 map quadrangle to the west of Latimojong Mountains (Ratman and Atmawinata,  
192 1993). Similar sequences of low-grade metasediments of Late Campanian-Late  
193 Maastrichtian age also occur in the South Arm of Sulawesi in the Bantimala and  
194 Barru areas (e.g. Balangbaru Formation; Sukamto, 1982; Hasan, 1991) and the Biru  
195 area (e.g. Marada Formation; van Leeuwen, 1981). They are considered to have  
196 formed in a fore-arc setting along the SE margin of Sundaland during NW-directed  
197 subduction in the Late Cretaceous (van Leeuwen and Muhardjo, 2005) and they  
198 overlie highly tectonized rocks of a Lower Cretaceous accretionary and ophiolite  
199 complex (van Leeuwen, 1981; Sukamto, 1982; Wakita et al., 1996; Maulana et al.,  
200 2010). These low-grade metasediments are clearly different to those originally  
201 described as the Latimojong Formation by Djuri and Sudjatmiko (1974) within the  
202 Latimojong region.

203

204 Other workers proposed the term “*Latimojong Complex*” for the rocks exposed in the  
205 Latimojong region (Coffield et al., 1993). This term was used to encompass two  
206 sequences: (1) unmetamorphosed sediments or very low grade metasediments,  
207 described as flysch or turbidites, which overlie: (2) strongly deformed low to high  
208 grade metamorphosed rocks, both of which were considered to exist in the  
209 Latimojong region. Based on our own observations in the Latimojong region, as well  
210 as other parts of western Sulawesi, we differentiate between these two sequences. We  
211 use the term ‘*Latimojong Metamorphic Complex*’ for the older, strongly  
212 deformed/metamorphosed rocks and ‘*Latimojong Formation*’ for the younger,  
213 unmetamorphosed or very low-grade metamorphosed sedimentary rocks.

214

215 The Latimojong Metamorphic Complex is exposed throughout the Latimojong  
216 Mountains; it is unclear whether the Latimojong Formation exists in the Latimojong  
217 region. Both sequences are considered to be Cretaceous (in a stratigraphic sense), with  
218 the Latimojong Formation unconformably overlying the Latimojong Metamorphic  
219 Complex. However, readers should note that no contact between the two units has  
220 been observed, and that there is no reliable age data available for these sequences in  
221 the Latimojong region. For example, these were originally assigned a Late Cretaceous  
222 age on the basis of Globotruncana found within claystone (Djuri and Sudjatmiko  
223 1974), but no localities for these fossils were reported. Later mapping reports by  
224 GRDC (Simandjuntak et al., 1991) refer back to Djuri and Sudjatmiko (1974), and  
225 also refer to Cretaceous aged fossils reported from grey limestones between Pasui and  
226 Rante Lemo by Brouwer (1934). These fossils include Orbitolina and Astrarea cf.  
227 Culumellata that were said to be potentially Cretaceous in age..

228

229 The Latimojong Metamorphic Complex includes multiply deformed quartz-  
230 muscovite-albite schist, glaucophane-lawsonite schist, graphitic schists and slate  
231 (Querubin and Walters 2011; this study). Meta-igneous rocks such as amphibolite,  
232 meta-gabbro and meta-granitoids are tectonically juxtaposed within parts of the  
233 Latimojong Metamorphic Complex. These could be mapped as part of the Latimojong  
234 Metamorphic Complex, but potentially represent younger rocks (e.g. the Lamasi  
235 Complex, Palopo Granite) that were tectonically juxtaposed with the older  
236 metamorphic sequences.

237

238 We assume that the Latimojong Metamorphic Complex is equivalent to the early Late  
239 Cretaceous medium-high grade metamorphic rocks exposed in South Sulawesi in the  
240 Bantimala and Barru areas (e.g. Wakita et al., 1996). We consider the Latimojong  
241 Formation was deposited unconformably on the Latimojong Metamorphic Complex  
242 and is equivalent in age to similar lithologies exposed in other parts of Western  
243 Sulawesi such as the Balangbaru and Marada formations (Sukanto and Simandjuntak,  
244 1983; Hasan, 1991; van Leeuwen and Muhardjo, 2005; Calvert and Hall, 2007; van  
245 Leeuwen et al., 2016). We are just not certain whether the Latimojong Formation  
246 exists within the Latimojong region.

247

248

### 249 3.2 The Lamasi Complex

250 Mafic to intermediate igneous rocks are exposed in the eastern Latimojong Mountains  
251 and close to the northwest coast of Bone Bay (Fig. 2 and Fig. 3). These were  
252 originally named the Lamasi Volcanics, and described as an Oligocene sequence of  
253 lava flows, basalts, andesites, volcanic breccia and volcanoclastics (Djuri and  
254 Sudjatmiko, 1974). Subsequent work demonstrated that the area originally mapped as  
255 basalts and basaltic andesites (Djuri and Sudjatmiko, 1974), also includes serpentinite,  
256 layered gabbro, isotropic gabbro, microdiorite, basaltic sheeted dykes, pillow lavas  
257 (with altered interstitial chert), dolerite, hyaloclastite, tuffs and volcanoclastic breccia  
258 (Coffield et al., 1993; Bergman et al., 1996). This suite of more mafic rocks was later  
259 re-named the Lamasi Complex (Coffield et al., 1993; Bergman et al., 1996). The  
260 basaltic rocks were interpreted to represent obducted MORB or back-arc oceanic crust  
261 as they have 'depleted' or MORB-like Sr and Nd isotopic ratios and REE  
262 characteristics (Bergman et al., 1996). Various isotopic data (K-Ar,  $^{40}\text{Ar}$ - $^{39}\text{Ar}$ , Rb-Sr  
263 and Sm-Nd) suggest Cretaceous to Oligocene ages (Priadi et al., 1994; Bergman et al.,  
264 1996). These ages are supported by field observations that show that these volcanic  
265 rocks are overlain by Lower to Middle Miocene marls and limestones (Djuri and  
266 Sudjatmiko, 1974). Similar lithologies are exposed in the Bone Mountains region,  
267 south of the Latimojong Mountains, where basalts, andesites and subordinate rhyolites  
268 are interbedded within middle Eocene to early Miocene clastics and carbonates (e.g.  
269 van Leeuwen et al., 2010).

270

271 Other workers reported K-Ar ages (19 Ma to 15 Ma) for basalts and andesites that



272 were said to be part of the Lamasi Volcanics (Priadi et al., 1994; Elberg and Foden,  
273 1999b). The ~15 Ma sample reported by Priadi et al., (1994) was a basaltic pillow  
274 lava. However, the sample analysed by Elberg and Foden (1999b) was from andesite  
275 float assumed to represent the Lamasi Complex. These ages are considerably younger  
276 than the Cretaceous-Eocene ages presented by Priadi et al. (1994) and Bergman et al.  
277 (1996). We suggest that these Miocene ages reflect a different magmatic event to  
278 those we classify as the Lamasi Complex.

279

### 280 3.3 Toraja Group (Eocene-Oligocene)

281 The Toraja Group is a c.1000m thick succession of locally folded terrestrial/marginal  
282 marine to shallow marine deposits. It was initially named the Toraja Formation with a  
283 type location in the Latimojong region (Djuri and Sudjarmiko, 1974) and was  
284 subdivided informally into two members (Djuri and Sudjarmiko, 1974; Coffield et al.,  
285 1993; Endaharto, 2000). The lowest member includes reddish-brown and grey shales,  
286 claystone and limestone as well as quartz sandstone, conglomerate and coal. The  
287 upper member has layers of white to grey limestone (Djuri and Sudjarmiko, 1974;  
288 Coffield et al., 1993; Bergman et al., 1996; Endaharto, 2000). The same lithologies  
289 and stratigraphic relationships are also observed in other parts of west Sulawesi  
290 (Wilson and Bosence, 1996; van Leeuwen and Muhandjo, 2005; Calvert and Hall,  
291 2007). They were later redefined as the Toraja Group, with the lower member named  
292 the Middle to Upper Eocene Kalumpang Formation and the inter-fingering/overlying  
293 carbonates assigned to the Middle Eocene to Upper Oligocene Budungbudung  
294 Formation (Calvert and Hall, 2007).

295

296 The Toraja Group has been interpreted as a terrestrial deltaic sequence in the  
297 Latimojong and Makale regions (Fig. 4), deposited unconformably above Mesozoic  
298 basement rocks (Coffield et al., 1993; Bergman et al., 1996; Calvert and Hall, 2007).  
299 The sediments have been interpreted as a syn-rift sequence deposited during rifting  
300 associated with extension in the Makassar Strait (Coffield et al., 1993; Bergman et al.,  
301 1996; Calvert and Hall, 2007). This model is supported by reports of quartz-  
302 dominated conglomerates at the base of the Toraja Group deposited during the early  
303 stages of graben development (van Leeuwen, 1981; Coffield et al., 1993; Calvert and  
304 Hall, 2007).

305

306 Foraminifera from the Toraja Group were initially assigned a Middle Eocene to  
307 Middle Miocene age (Djuri and Sudjatmiko, 1974) but the group is now considered to  
308 have been deposited between the Eocene and Oligocene (Coffield et al., 1993; Calvert  
309 and Hall, 2007). Thin nummulitic limestones deposited on tilted fault blocks in the  
310 region mark a marine transgression during the Middle Eocene, including at the base of  
311 the Budunghbung Formation (Coffield et al., 1993; Calvert and Hall, 2007).

312

### 313 3.4 Makale Formation (Lower to Middle Miocene)

314 The Makale Formation is a 500m to 1000m-thick sequence of interbedded reef  
315 limestone and marl that conformably overlies the Toraja Group (Djuri and  
316 Sudkatmiko, 1974; Sukanto and Simandjuntak, 1983). It is considered to be the  
317 regional stratigraphic equivalent of the Middle Miocene to Lower Pliocene Tacipi  
318 Limestone (found to the east of the Walanae Fault), with the underlying Toraja Group  
319 being equivalent to the Tonasa Limestone (Wilson and Bosence, 1996). The Makale  
320 Formation probably developed as a series of pinnacle/patch reefs, similar to that  
321 proposed for the Tacipi Limestone (e.g. Grainge and Davies 1985; Coffield et al.,  
322 1993; Wilson and Bosence, 1996; Ascaria, 1997).

323

324 Reef limestones of the Makale Formation cap many of the summits in the Latimojong  
325 and Makale regions with recognizable steep cliffs and karst topography (Fig. 5). This  
326 formation is thought to represent a widespread fully marine carbonate platform. Its  
327 age is somewhat debated, with Early to Middle Miocene (Djuri and Sudkatmiko,  
328 1974), Late Oligocene to Middle Miocene (Baharduddin and Harahap, 2000) and  
329 Eocene to Middle Miocene (Coffield et al., 1993; Endaharto, 2000) ages proposed on  
330 the basis of different fossil assemblages. The base of the formation has been described  
331 as concealed or faulted (Djuri and Sudkatmiko, 1974), and as conformable on the  
332 Toraja Group (Endaharto, 2000). The top of the formation has been eroded and  
333 overlying units have been removed (Djuri and Sudkatmiko, 1974). The basal part is  
334 overlain by deeper marine, outer shelf platform limestone (dominantly mudstones and  
335 wackestones) (Coffield et al., 1993).

336

### 337 3.5 Igneous Rocks

#### 338 *3.5.1 Oligocene Intrusives*

339 Granites and granodiorite named the Kambuno Granite cross-cut Cenozoic volcanic

340 breccias near Rantepao. These granites yielded a K-Ar age of 29.9 Ma (Priadi et al.,  
341 1994). Little information exists about location and extent of these granitoids, except  
342 that they are found ~5 km north of Sadang Village along the Sadang River.

343

#### 344 *3.5.2 Mio-Pliocene Extrusives (Enrekang Volcanic Series)*

345 The Enrekang Volcanic Series is found to the west of the Latimojong Mountains and  
346 covers large parts of central-West Sulawesi (Coffield et al., 1993). It consists of  
347 volcanoclastic sandstones and conglomerates interbedded with tuffs and lava flows  
348 (e.g. Fig. 6). These sequences are ~500m to ~1000m thick and were deposited during  
349 the Middle Miocene to Pliocene, based on foraminifera and nannofossils in  
350 sedimentary rocks (Djuri and Sudkatmiko, 1974; Maryanto, 2002) and ca. 13 Ma to  
351 2.4 Ma ages determined from K-Ar dating of biotite (Bergman et al., 1996; Polvé et  
352 al., 1997; Elburg and Foden, 1999b). The volcanic rocks are exclusively potassic to  
353 ultra-potassic in composition (e.g. Polvé et al., 1997) and have been considered  
354 equivalent to the Camba Volcanics in the South Arm of Sulawesi (e.g. Sukanto,  
355 1982; Sukanto and Simandjuntak, 1983; Yuwono et al., 1988; Wilson and Bosence,  
356 1996).

357

#### 358 *3.5.3 Mio-Pliocene Intrusives*

359 Mio-Pliocene intrusive rocks are found in the Latimojong region (Djuri and  
360 Sudkatmiko, 1974; Coffield et al., 1993; Priadi et al., 1994; Bergman et al., 1996;  
361 Polvé et al., 1997). These are considered to be the plutonic equivalents of the Middle  
362 Miocene to Pliocene Enrekang Volcanic Series (Coffield et al., 1993; Bergman et al.,  
363 1996). Rb-Sr, Nd-Sm and U-Pb isotopic data were used to infer that these magmatic  
364 rocks melted a Late Proterozoic to Early Paleozoic crustal source during continent-  
365 continent collision (Bergman et al., 1996).

366

367 The granitoids exposed in the Latimojong region are known as the Palopo Granite  
368 (Simandjuntak et al., 1991; Priadi et al., 1994) or Palopo Pluton (Bergman et al.,  
369 1996). These granitoids intrude, or are in fault contact, with the Latimojong  
370 Metamorphic Complex, the Lamasi Complex and the Toraja Group (Djuri and  
371 Sudjatmiko, 1974; Simandjuntak et al., 1991; Priadi et al., 1994; Bergman et al.,  
372 1996). The Palopo Granite consists of medium- to coarse-grained granite and  
373 granodiorite (Simandjuntak et al., 1991) (Fig. 7). The granite is composed of quartz,

374 orthoclase and minor hornblende, while the granodiorite consists of larger  
375 phenocrysts of plagioclase and K-feldspar within a quartz, feldspar, hornblende and  
376 biotite groundmass (Simandjuntak et al., 1991). The mafic minerals in both granitoids  
377 are commonly chloritized (Simandjuntak et al., 1991).

378

379 K-Ar dates of the Palopo Granite were obtained from tonalite, granodiorite and a  
380 granite dyke in the Palopo region and yielded ages of 5.0 Ma, 5.5 Ma and 8.1 Ma  
381 respectively (Sukamto, 1975). These ages were reproduced in later K-Ar analyses of  
382 the Palopo Granite (e.g. Priadi et al., 1994; Bergman et al., 1996; Polvé et al., 1997).  
383 Bergman et al. (1996) also obtained Rb-Sr and Sm-Nd whole rock analyses, as well as  
384 a U-Pb ID-TIMS date of zircon, together with fission track analyses of apatite, zircon  
385 and titanite for several Palopo Granite samples. The ages that were obtained from  
386 these various analyses range between ~11 Ma and ~2 Ma. The one U-Pb zircon age  
387 from the Palopo Granite (5.4 Ma) was the same as K-Ar age ( $5.4 \pm 0.4$  Ma) from the  
388 same sample (Bergman et al., 1996). This is highly unusual, and indicates either that  
389 there was a problem with one (or both) of these analyses, or that the granite must have  
390 cooled rapidly on emplacement.

391

### 392 3.6 Upper Miocene to Recent clastic deposits

393 The sedimentary rocks described above are overlain by Upper Miocene to Pliocene  
394 mudstones, siltstones, sandstones and conglomerates of the Walanae Formation  
395 (Grainge and Davies, 1985) (Fig. 8), as well up to c.100 m of recent alluvium, clay,  
396 silt, sand, gravel and limestone (Djuri and Sudjarmiko, 1974).

397

## 398 **4. Mapping and sample details**

399 The work we present is largely a summary of several field campaigns conducted  
400 during 1995-1997 (AJB/JS) and in 2012 (LTW/RH). The majority of the results that  
401 are presented here are from fieldwork conducted in September 2012, however, we  
402 relied on the Southeast Asia Research Group's sample catalogue as well as existing  
403 maps and thin sections to develop a revised map of the Latimojong region (Fig. 2).  
404 Further details on the field observations and lithologies observed are included in  
405 Supplementary File 1. This map was developed using a GIS using high-resolution,  
406 remotely sensed data and aerial imagery to develop a better understanding of the  
407 regional structural grain and potential contacts between units (Fig. 2). These data were

408 highly valuable as we did not locate many contacts between geological units in the  
409 field. The majority of the contacts that we did observe were sub-vertical and these are  
410 likely to be associated with phases of strike-slip faulting during the Late Miocene to  
411 Recent.

412

413 Several spot samples of chert, carbonate and volcanoclastic rocks were sampled from  
414 the Latimojong Metamorphic Complex, Lamasi Complex, Toraja Formation,  
415 Enrekang Volcanic Series and Makale Formation for radiolarian and foraminiferal  
416 biostratigraphy (Fig. 2). The results for each sequence/formation are discussed below  
417 (Section 5). Various granitic and volcanic rocks were also sampled in the area (Fig. 2,  
418 Fig. 6, Fig. 7, Fig. 9). Eleven representative samples were selected for geochemical  
419 analyses. Eight of these samples were then selected for zircon U-Pb dating. The  
420 primary aim of the geochemical and isotopic analyses was to determine if certain  
421 compositions were generated at specific times. In several cases, we were able to  
422 obtain samples of dykes that cross-cut older sedimentary and igneous rocks that have  
423 allowed us to limit the timing of deposition/emplacement of particular units.

424

425

## 426 **5. Biostratigraphic results**

### 427 5.1 Chert from the Latimojong Metamorphic Complex or Lamasi Complex

428 Several samples of chert intercalated with pillow basalts from the Lamasi Complex  
429 (e.g. Fig. 3) were sampled, but no radiolarians could be identified due to extensive  
430 veining and recrystallization. Identifiable radiolarians were extracted from a 0.5m  
431 boulder of red chert found in a river to the west of the Latimojong Mountains (Fig. 2  
432 and Fig. 10). This sample contained several poorly preserved radiolarian tests,  
433 including *Stichomitra* cf. *japonica*, *Xitus* cf. *clava*, *Thanarla* cf. *pulchra*, *Distylocapsa*  
434 sp., *Hiscocapsa* sp. and *Dictyomitra* spp. (Fig. 10), indicating an Early Cretaceous  
435 (possibly Albian) age (O'Dogherty, 2009). The chert sample was found alongside  
436 other river float, including pieces of schist, quartzite, sandstone, diorite and deformed  
437 igneous breccia. We suspect this most likely represents material from the Latimojong  
438 Metamorphic Complex.

439

### 440 5.2 Foraminifera from the Toraja Group, Makale Formation and Enrekang Volcanics

441 Benthic and planktonic foraminifera from eighteen samples of packstone and

442 wackestones from the Latimojong region (Fig. 2) were dated based on BouDagher-  
443 Fadel (2008, 2013), and assigned ages using the time scale of Gradstein et al. (2012).  
444 The age range of each of these samples and the stratigraphic unit they are assigned to  
445 (Toraja Group, Makale Formation and Enrekang Volcanic Series; Djuri and  
446 Sadjtmiko, 1974; Calvert and Hall, 2007) are summarised in Fig. 11. The location of  
447 each of these samples is shown on the geological map in Fig. 2. Details of the sample  
448 location and foraminifera identified in each sample are presented in Supp. File 1 and  
449 the interactive map file.

450

#### 451 *5.2.1 The Toraja Group*

452 Foraminifera analyses indicate that the Toraja Group is Eocene to Oligocene  
453 (Ypresian to Chattian; 56–23 Ma) and was deposited in a reef and inner neritic setting  
454 in the Latimojong region (Fig. 11 and Supp. File 1 and 2). Many of the samples  
455 record age ranges that do not overlap (e.g. K12-10, K12-13, K12-17, PA178, PA277),  
456 while the timing of deposition of other samples were poorly constrained (e.g. K12-  
457 22A, PA58, PA59) (Fig 10 and Supp. File 1).

458

#### 459 *5.2.2 The Makale Formation*

460 Five samples of foraminifera-bearing packstones and wackestones (PA56, PA63,  
461 PA184, K12-20A, K12-20B) from the Makale Formation (Fig. 2) have Miocene ages  
462 of Burdigalian and Serravallian (20.5–11.5 Ma) (Fig. 11). These assemblages, along  
463 with those obtained from the Toraja Group, indicate that there was potentially a  
464 minimum of ~2.5 Myr. to a maximum of 15 Myr. without significant carbonate  
465 deposition (Fig. 11), assuming no sampling bias.

466

#### 467 *5.2.3 Enrekang Volcanic Series*

468 Two samples of indurated foraminifera-bearing wackestone (K12-20A and -20B)  
469 were collected from the Enrekang Volcanic Series. Sample K12-20A provided only a  
470 wide Cenozoic age as the foraminifera could be identified only to genus level (e.g.  
471 *Operculina sp.*, *Amphistegina sp.*, *Globigerina sp.*), but sample K12-20B yielded a  
472 Late Miocene–Early Pliocene age. The age of this sample is interpreted to indicate  
473 that the Enrekang Volcanic Series was deposited at some time between the Tortonian  
474 and Zanclean (11.5 Ma to 3.5 Ma) (Fig. 11) in the Latimojong region.

475

476 **6. Geochemistry and isotopic dating of igneous rocks**

477 6.1 Methodology: Geochemistry and Isotopic Dating

478 *6.1.1 Sample Processing*

479 Samples were crushed into 2-5 cm<sup>3</sup> pieces using a jaw crusher. The crushed aggregate  
480 was rinsed to remove any potential contaminants and left to dry before being  
481 pulverised to a fine-powder using a tungsten carbide swing mill. The aggregate was  
482 sieved using a disposable nylon mesh to capture material that was <250 µm. This was  
483 'deslimed' to remove the finest grain size fraction. A zircon concentrate was obtained  
484 by processing this material through high-density liquids and magnetic separation.  
485 Zircons were hand picked and set in 25 mm epoxy disks along with the Temora-2 U-  
486 Pb zircon standard (Black et al., 2004). The mount was polished to expose the mid-  
487 sections of the grains and was examined with an optical microscope and photographed  
488 under transmitted and reflected light. All zircons were then imaged with a Robinson  
489 Cathodoluminescence (CL) detector fitted to a JEOL JSM 6610-A scanning electron  
490 microscope (SEM) at the Research School of Earth Sciences, The Australian National  
491 University (ANU).

492

493 *6.1.2 Zircon Geochronology*

494 U-Pb isotopic measurements were collected from zircons from eight samples using a  
495 sensitive high resolution ion microprobe (SHRIMP-RG) at the Research School of  
496 Earth Sciences, ANU. The CL imagery as well as reflected and transmitted light  
497 microscopy were used to identify zircon cores and growth rims that were suitable for  
498 dating. Standard zircon SL13 (U = 238 ppm; Th = 21 ppm; Claoué-Long et al., 1995)  
499 was used to calibrate the U and Th concentrations and Pb/U ratios were corrected for  
500 instrumental inter-element fractionation using the ratios measured on the standard  
501 zircon Temora 2 (416.8 ± 1.3 Ma; Black et al., 2004). One analysis of a Temora  
502 zircon was made for every four analyses of unknowns. The data were reduced in a  
503 manner similar to that described by Williams (1998, and references therein), using the  
504 SQUID 2 Excel macro (Ludwig, 2009) and these were interrogated further using  
505 Isoplot (Ludwig, 2003). The decay constants recommended by the IUGS  
506 Subcommittee on Geochronology (as given in Steiger and Jäger, 1977) were used in  
507 age calculations. Uncertainties given for individual U-Pb analyses (ratios and ages)  
508 are at the 1-sigma level. All age results less than 800 Ma are reported using <sup>207</sup>Pb  
509 corrected <sup>206</sup>Pb/<sup>238</sup>U system because of the uncertainties associated with low <sup>204</sup>Pb,

510  $^{207}\text{Pb}$  and  $^{208}\text{Pb}$  yields from zircons of this age. Ages >800 Ma are reported using  
511  $^{204}\text{Pb}$  corrected  $^{207}\text{Pb}/^{206}\text{Pb}$  system. We assessed the common Pb concentrations  
512 recorded for each of the analyses for each sample. We found that rejecting analyses  
513 with >2% common Pb made no appreciable difference to the weighted mean age  
514 calculated for each sample, but it did influence the MSWD associated with this age.  
515 The uranium concentrations and age obtained for each zircon were examined to assess  
516 for potential matrix effects associated with high-U zircon sample (e.g. White and  
517 Ireland, 2012). This issue was only observed in one sample (K12-6B), and in this case  
518 analyses that recorded U concentrations >5000 ppm were rejected from the  
519 calculation of the weighted mean age.

520

### 521 *6.1.3 Geochemistry*

522 An aliquot of each milled rock sample (described above in 4.1.1) was collected prior  
523 to being sieved. The aliquot was milled further and made into glass disks and pellets  
524 for whole rock major and trace element geochemical analyses. The major and trace  
525 element data were collected using a Panalytical Axios WDS XRF spectrometer at  
526 Royal Holloway, University of London.

527

## 528 **7. Zircon Geochronology Results**

529 The eight variably deformed granitoids and volcanic to hypabyssal rocks were dated  
530 from the Latimojong region. The geochronology results are discussed below  
531 according to lithology and age, ordered youngest to oldest. These results are  
532 summarised in Table 1. Tera Wasserburg concordia diagrams and relative probability  
533 age plots for the samples are shown in Fig. 12 and Fig. 13 respectively.

534

### 535 7.1 Enrekang Volcanic Series

536 Three dacitic samples yielded latest Miocene to Pliocene zircon U-Pb ages and are  
537 classified as the Enrekang Volcanic Series. The youngest sample is a fine-grained  
538 felsic dyke (K12-33B) that cross-cuts a schist of the Latimojong Complex (Fig. 6a).  
539 SHRIMP U-Pb analyses of five individual zircon crystals were appreciably older  
540 (1432 Ma, 235 Ma, 213 Ma, 38 Ma, 35.8 Ma) compared to the dominant 3.9 Ma age  
541 population. These older analyses are interpreted to be inherited ages from the partially  
542 melted country rocks. The other fifteen zircon analyses are interpreted as magmatic  
543 ages. Four of these analyses yielded >2% common Pb and were thus rejected from



544 further consideration. The remaining 11 analyses yielded a weighted mean age of 3.9  
545  $\pm 0.1$  Ma (MSWD = 1.0) and is interpreted as the age of crystallization of this sample.

546

547 The second dacite sample (K12-21A) from the Enrekang Volcanic Series has a  
548 weighted mean age of  $6.8 \pm 0.1$  Ma (MSWD = 2.7) ( $n = 24$  analyses). This sample  
549 also contained two inherited zircon cores (136 Ma and 9.1 Ma).

550

551 The third sample of dacite (K12-27) from the Enrekang Volcanic Series yielded a  
552 weighted mean age of  $7.5 \pm 0.1$  Ma (MSWD = 1.5) ( $n = 15$ ). There were several  
553 inherited ages (193 Ma, 38.3 Ma, 37.7 Ma, 35.7 Ma, 36.3 Ma, 36.5 Ma and 34.5 Ma).

554 The inherited analyses between 38–34 Ma clearly define one age population and yield  
555 a weighted mean age of  $36.5 \pm 0.7$  Ma (MSWD = 1.2) ( $n = 6$ ). All of these 38–34 Ma  
556 analyses were obtained from zircon cores, or zircon grains that showed no evidence of  
557 overgrowths. This age was also recorded by the Enrekang Volcanic Series dyke  
558 (sample K12-33B) discussed above and a sample that we propose is part of the  
559 Lamasi Volcanics (K12-11B) (Fig. 13a, 13d, 13h) discussed below. We therefore  
560 interpret this 36.5 Ma age to record Eocene magmatism in Western Sulawesi,  
561 preserved in zircon xenocrysts sampled by the Pliocene dacitic magma.

562

## 563 7.2 Palopo Granite

564 Zircons were extracted from one undeformed sample (K12-4B) and two deformed  
565 samples (K12-35B and K12-6B) of granodiorite from the Palopo Granite. These  
566 samples yielded weighted mean ages of:

- 567 •  $5.0 \pm 0.1$  Ma (MSWD = 2.1) ( $n = 16$ ) [K12-4B].
- 568 •  $6.3 \pm 0.1$  Ma (MSWD = 1.0) ( $n = 14$ ) [K12-35B].
- 569 •  $6.4 \pm 0.2$  Ma (MSWD = 4.8) ( $n = 9$ ) [K12-6B].

570

571 Each of these granodiorite samples recorded inherited ages. Only one inherited age  
572 (1728 Ma) was obtained from sample K12-4B. Multiple inherited ages [309 Ma, 265  
573 Ma, 219 Ma, 195 Ma and 102 Ma] and [1460 Ma, 373 Ma, 260 Ma, 131 Ma, 102 Ma,  
574 9.8 Ma and 8.3 Ma] were obtained from samples K12-35B and K12-6B respectively.

575

## 576 7.3 Bua Rhyolite Dyke [Lamasi Complex?] (Sample: K12-7-31)

577 Zircons were extracted from a rhyolite dyke that cross-cuts basalts from the Lamasi  
578 Volcanics (Fig. 9). We refer to this rhyolitic dyke as the ‘Bua Rhyolite’ as it outcrops  
579 near Bua Village (e.g. Fig. 2 and Fig. 9). The magmatic zircons in this sample exhibit  
580 very low uranium and thorium concentrations ([U]: 15–108 ppm and [Th]: 2–47 ppm)  
581 and most grains recorded common Pb concentrations >2% (Supp. Data File 3). If  
582 these are excluded, the remaining analyses yield a weighted mean age of 25.0 Ma ±  
583 0.7 Ma (MSWD = 0.5) (n = 4). This age is effectively the same as a weighted mean  
584 age that includes all of the high common Pb analyses [25.0 Ma ± 0.3 Ma (MSWD =  
585 1.1) (n = 23 analyses)]. The Bua Rhyolite is therefore interpreted to have crystallized  
586 at 25.0 Ma ± 0.7 Ma and this provides a minimum age for the Lamasi Complex. The  
587 Bua Rhyolite Dyke also contains inherited Paleoproterozoic (2474 Ma) and Archean  
588 (2680 Ma) zircon cores.

589

#### 590 7.4 Andesite [Lamasi Complex] (Sample: K12-11B)

591 Several zircons were extracted from one sample of andesite (K12-11B) and we were  
592 able to date twelve grains from this sample. Four of the analyses were between 37 Ma  
593 and 40 Ma. These yielded a weighted mean age of 38.2 ± 1.3 Ma (MSWD = 2.2) and  
594 we interpret this as the age of crystallization of this sample. The remaining analyses  
595 are interpreted as inherited ages (1717 Ma, 102 Ma, 101 Ma, 99.6 Ma, 99.2 Ma, 94.2  
596 Ma, 89.6 Ma, 51 Ma and 44 Ma). We interpret this sample to be part of the Lamasi  
597 Complex.

598

### 599 **8. Geochemistry results for the igneous rocks**

600 The geochemical data obtained from the igneous rocks indicate that there are several  
601 distinct populations with different whole rock chemistries. While many of the  
602 volcanic samples show evidence of moderate to substantial alteration, three broad  
603 compositional groups can be identified (Fig. 14a). Samples from the Enrekang  
604 Volcanic Series and the Palopo Granite plot within the dacite/granodiorite field (Fig.  
605 14a). Two analyses plot outside this dominant group represented by the Enrekang  
606 Volcanic Series and Palopo Granite. These ‘outliers’ represent an altered andesite  
607 (K12-11B) found within a strike-slip fault zone and the Bua Rhyolite Dyke (K12-31)  
608 that cross-cuts basalts of the Lamasi Volcanics.

609

610 The broad differences in geochemistry are also reflected in other geochemical indices

611 (e.g. Frost et al., 2001; Frost and Frost 2008) and discrimination plots (e.g. Modified  
612 Alkali Lime vs. SiO<sub>2</sub>; FeO/(FeO+MgO) vs. SiO<sub>2</sub> and Aluminium Saturation Index  
613 (ASI) vs. SiO<sub>2</sub>) (Fig. 14b-d) (Supp. Data File 4). The geochemical groupings also  
614 correspond to different crystallization ages (cf. Fig. 14 and the geochronology results  
615 presented in Section 7).

616

## 617 **9. Discussion**

### 618 9.1 Revised Geological Map and Stratigraphy

619 Our field investigations have shown considerable differences from earlier geological  
620 maps of the Latimojong region (e.g. Djuri and Sudjarmiko, 1974; Simandjuntak et al.,  
621 1991; Bergman et al. 1996) (Fig. 2). Some of these discrepancies reflect the location  
622 of our traverses that sampled new exposures (e.g. new road cuttings) provided as the  
623 region has been developed. Our fieldwork and access to high-resolution remotely  
624 sensed data enabled a revised geological map to be produced (Fig. 2). The new  
625 biostratigraphic and isotopic dating provide some limitations on the age of deposition,  
626 igneous activity and deformation in the region. From what we observed, we consider  
627 that many of the thrust contacts proposed by Bergman et al. (1996) could equally be  
628 normal faults, strike-slip faults or stratigraphic (conformable or unconformable)  
629 contacts. Because of the terrain and vegetation almost all contacts are interpreted.

630

#### 631 *9.1.1 The Latimojong Metamorphic Complex*

632 There are no precise age controls on the age of the Latimojong Metamorphic  
633 Complex. Our mapping of the region has reduced its area compared to earlier  
634 geological maps (Fig. 2) (e.g. Djuri and Sudjarmiko, 1974). The metamorphic rocks  
635 are assumed to be Cretaceous as they are similar to lithologies that have been dated in  
636 Barru and Bantimala (e.g. Wakita et al., 1996; Parkinson et al., 1998). The Aptian-  
637 Albian age radiolaria that we identified in a piece of chert float, found to the west of  
638 the Latimojong Mountains, provides some support for this assumption. More support  
639 for this is provided by 128-123 Ma zircon fission track ages obtained from two  
640 metasediment samples collected from the western edge of the Latimojong Mountains  
641 as well as a Cretaceous (114 ± 2 Ma) K/Ar age obtained from white mica in an  
642 Oligocene sandstone from the Latimojong region (Bergman et al., 1996). When  
643 considered together, these Cretaceous ages may indicate that the Latimojong  
644 Metamorphic Complex formed in the Early Cretaceous. Future isotopic age data (e.g.

645  $^{40}\text{Ar}$ - $^{39}\text{Ar}$  analyses of mica and U-Pb dating of zircon) from Latimojong Metamorphic  
646 Complex schists should provide more clarity as to the age of metamorphism and the  
647 age spectra of the protolith.

648

#### 649 *9.1.2 The Lamasi Complex*

650 The rocks of the Lamasi Complex are predominantly found to the east of the  
651 Latimojong Mountains (Fig. 2). We assigned the majority of mafic volcanic (e.g.  
652 basalt) and intrusive rocks (gabbros) that occur east of the Latimojong Mountains to  
653 the Lamasi Complex. We interpret that the  $25.0 \pm 0.7$  Ma date obtained from a  
654 rhyolite dyke (the Bua Rhyolite) that cross-cuts basalt (Fig. 9) provides a minimum  
655 limit on the age of the Lamasi Complex. A similar age (29.9 Ma) was obtained from a  
656 K-Ar age for granite that cross-cut Cenozoic volcanic breccias near Rantepao (Priadi  
657 et al., 1994). Together, these two ages from felsic rocks that crosscut mafic rocks  
658 provide a minimum time estimate for the emplacement of the Lamasi Complex  
659 volcanics. We therefore suspect that the  $\sim 38.2 \pm 1.3$  Ma age obtained from a highly  
660 altered andesite (Sample: K12-11B) reflects a phase of volcanism associated with the  
661 Lamasi Complex. The evidence for this Eocene-Oligocene phase of magmatism is  
662 also supported by ages obtained from inherited zircons from dacites of the Enrekang  
663 Volcanic Series (e.g. K12-27: Fig. 13f). Similar ages have also been reported from  
664 earlier K-Ar dating (e.g. Priadi et al., 1994) and from igneous rocks further north in  
665 Central Sulawesi and Sulawesi's "Neck" (Hennig et al., 2016).

666

667 We speculate that the gabbros and ultramafic rocks found in this area are part of the  
668 Latimojong Metamorphic Complex and are of Cretaceous age (although this is not  
669 reflected in the geological map shown in Fig. 2). Similar ultramafic rocks are found  
670 associated with Cretaceous medium- to high-grade metamorphic rocks in the Barru  
671 and Bantimala regions in southern Sulawesi (e.g. Wakita et al., 1996; Parkinson et al.,  
672 1998).

673

674 The isotopic and biostratigraphic ages obtained from the Lamasi Complex and the  
675 Toraja Group indicate that the lowermost sediments of the Toraja Group were  
676 deposited at the same time as the igneous rocks of the Lamasi Complex were  
677 crystallizing during the Eocene (Fig. 15). Continued deposition of the Toraja Group  
678 likely means that these sediments stratigraphically overlie the Lamasi Complex in

679 places. We could not verify this stratigraphic relationship in the Latimojong region  
680 (partly due to the terrain, vegetation cover as well as the numerous strike-slip faults).  
681 However, this stratigraphic relationship is observed in the Lariang and Karama  
682 regions (Calvert and Hall, 2007). Eocene volcanics are also considered to represent  
683 the acoustic basement in the East Sengkang Basin (Grainge and Davies, 1985), which  
684 is directly to the south of the Latimojong region. The Lamasi Complex may also  
685 correspond with the similar volcanics found within the mid- to late Eocene Matajang  
686 Formation (Group B) in the Bone Mountains region. Considering this widespread  
687 basaltic-andesitic volcanism, the Lamasi Complex may represent Eocene-Oligocene  
688 arc/back-arc volcanic rocks obducted during the Early to Middle Miocene and/or  
689 translated by movement along regional faults (e.g. Bergman et al., 1996; van Leeuwen  
690 et al., 2010).

691

### 692 *9.1.3 Toraja Group*

693 The biostratigraphic data obtained in this study indicate that the sedimentary rocks of  
694 the Toraja Group were deposited during the Eocene (from the Ypresian) and  
695 Oligocene (to the Chattian). This is largely in agreement with other work conducted in  
696 the region and further afield (e.g. Coffield et al., 1993; Calvert and Hall, 2007).  
697 However, all previous work indicates the Toraja Group was deposited between the  
698 Middle Eocene and Oligocene, while one of our samples extends this range to the  
699 Ypresian (Sample: K12-18). To our knowledge, there are no earlier reports of early  
700 Eocene fossils for the Toraja Group, so this age is potentially quite important. While  
701 this age was obtained from an isolated spot sample, we are confident of the age  
702 assigned to this particular sample on the basis of the foraminifera present. This new  
703 piece of information indicates evidence of shallow marine/reef conditions at c. 54–52  
704 Ma. This may represent a marine incursion during the Early Eocene (e.g. Fig. 11 and  
705 Fig. 15), similar to the thin layer of nummulitic carbonates deposited during the  
706 Middle Eocene at the base of the Budungbudung Formation found northwest of the  
707 Latimojong region (e.g. Calvert and Hall, 2007). The Toraja Group and associated  
708 sequences from other parts of western Sulawesi indicate that shallow marine  
709 carbonate deposition became more widespread during later parts of the Eocene and  
710 Oligocene (Sukanto and Simandjuntak, 1983; Coffield et al., 1993; Wilson and  
711 Bosence, 1996; Bergman et al., 1996; Calvert and Hall, 2007).

712

713 *9.1.4 Makale Formation*

714 Our results from several spot samples indicate that the carbonates of the Makale  
715 Formation were deposited during the Early to Middle Miocene (Burdigalian to  
716 Serravallian) (Fig. 11 and Fig. 15). These ages are in agreement with the work of  
717 Djuri and Sudkatmiko (1974). We consider the Eocene and Oligocene ages reported  
718 by other workers (see Section 3.4) were obtained from the Toraja Group, rather than  
719 the Makale Formation (e.g. Fig. 15). Our primary justification for dating the Makale  
720 Formation as Early to Middle Miocene in age, and the Toraja Group as Eocene to  
721 Oligocene in age is based on the pattern of outcrops that emerged through mapping  
722 (Fig. 2) and because the ages obtained from foraminifera show that there could have  
723 been a ~2.5 Ma break in deposition during the earliest Miocene (Aquitania) (Fig. 11  
724 and Fig. 15). The ages we propose for the Makale Formation support it being the  
725 stratigraphic equivalent of the Tacipi Limestone located further to the south (e.g. see  
726 Section 3.4 for further details)..

727

728 *9.1.5 Enrekang Volcanic Series and the Palopo Granite*

729 The Enrekang Volcanic Series was used by Coffield et al., (1993) to group several  
730 formations of high-K volcanics together (the Sekata Formation and the Adang, Sesean  
731 and Talaya volcanics). None of these formations have been studied in detail, but some  
732 geochemical, isotopic and radiometric age data exist (Priadi et al., 1994; Bergman et  
733 al., 1996; Elburg and Foden 1999). These data indicate that the Enrekang Volcanic  
734 Series consists of stratovolcano and volcanic apron successions with various  
735 pyroclastic and volcanoclastic deposits that were deposited between 13.1 Ma and 2.4  
736 Ma (e.g. Priadi et al., 1994; Bergman et al., 1996). In the Latimojong region, we dated  
737 two dacites that were emplaced between 6-8 Ma as well as a 3.9 Ma felsic dyke that  
738 cross-cut part of the Latimojong Metamorphic Complex. On the basis of their age,  
739 geochemistry and petrology, we classified these dacites as being part of the Enrekang  
740 Volcanic Series. These results were compared alongside the biostratigraphic ages  
741 obtained from foraminifera in two samples from the Enrekang Volcanic Series (K12-  
742 22B) (Fig. 11). The overlap between the ages from foraminifera and those obtained  
743 from U-Pb isotopic analyses of zircons define an age range of 8.0 Ma to 3.6 Ma for  
744 the magmatism and volcanoclastic sedimentation of the Enrekang Volcanic Series (i.e.  
745 mid-Tortonian to Zanclean) (Fig. 15). Readers should note however, that all of these  
746 ages represent “spot samples”, so the true age range for this sequence may be broader.

747

748 Interestingly, the dacites and felsic dyke yield similar ages and compositions to the  
749 Palopo Granite (Fig. 12–14) and it is possible that these are the plutonic and volcanic  
750 equivalents of one another. Geochemically, the Enrekang Volcanic Series are similar  
751 to the Palopo Granite, apart from two dacite samples (K12-21A/21B: taken from the  
752 same outcrop) that are metaluminous and have higher K contents than the granitoids.  
753 The geochemical data obtained from the Palopo Granite indicate these are high-K,  
754 magnesian, peraluminous and calc-alkaline to alkali-calcic granitoids. These results  
755 largely replicate the earlier work of Priadi et al., (1994) and indicate the granitoids fit  
756 within Sulawesi's Mio-Pliocene high-K calc-alkaline ("CAK") granitoid belt (e.g.  
757 Polvé et al. (1997); Hennig et al., 2016)).

758

### 759 9.2 Post-crystallisation deformation

760 Several samples of the Palopo Granite exhibit mylonitic fabrics that developed after  
761 the crystallization of the granite. This is confirmed from the microstructures, for  
762 example brittle-fracturing and mechanically induced grain-size reduction of feldspars  
763 and recrystallized quartz. The U-Pb SHRIMP zircon ages of c. 6.3 Ma obtained from  
764 deformed granodiorite (e.g. K12-6B and K12-35B) compared to 5.0 Ma from  
765 undeformed granodiorite (K12-4B) brackets the timing of mylonitization to between  
766 6.3 Ma and 5.0 Ma. These mylonites are steeply dipping and record strike-slip  
767 deformation, and we consider that these may reflect the westerly continuation of the  
768 Kolaka Fault Zone (Fig. 2). An age of  $4.4 \pm 0.2$  Ma from an undeformed dacite within  
769 the Kolaka Fault Zone, was interpreted as being injected at the same time as fault  
770 movement or after faulting had ceased (White et al., 2014). If the Kolaka Fault Zone  
771 does extend from Kolaka, across Bone Bay, and into the Latimojong region (e.g. Fig.  
772 1 and 2: Camplin and Hall, 2014; White et al., 2014), then the age of the deformed  
773 (~6.3 Ma) vs. undeformed (~5.0 Ma) granodiorites from the Palopo Granite provides  
774 a tighter limit on the timing of movement along the Kolaka Fault (at least on the  
775 western side of Bone Bay) than that proposed by White et al., (2014). Additional  
776 thermochronological analyses and petrographic investigations are underway to  
777 constrain the timing of this fault movement.

778

### 779 9.3 Basement Age

780 Rb-Sr, Nd-Sm and U-Pb isotopic data were used to infer that the Palopo Granite

781 melted a Late Proterozoic to Early Paleozoic crustal source during continent-continent  
782 collision (Bergman et al., 1996). The source interpretation is supported by the  
783 inherited ages obtained from zircon cores within granitic and volcanic rocks in this  
784 study, and in other parts of Central Sulawesi, Southeast Arm and the Neck (White et  
785 al., 2014; Hennig et al., 2016; van Leeuwen et al., 2016). The inherited ages most  
786 likely represent the remains of igneous and sedimentary rocks that were partially  
787 melted to produce the Palopo Granite and Enrekang Volcanic Series. These do not  
788 necessarily require a basement age of Late Proterozoic to Early Paleozoic, but  
789 indicate that there are Proterozoic and Paleozoic zircons within the basement rocks of  
790 central–west Sulawesi.

791

#### 792 9.4 Tectonic Evolution

793 Western Sulawesi (including the Latimojong region) has been interpreted to have  
794 developed in a foreland setting within a westward-verging orogenic wedge at the  
795 eastern margin of Sundaland between the Eocene to Pliocene (Coffield et al., 1993;  
796 Bergman et al., 1996). This model proposed that the Mio-Pliocene magmatic rocks  
797 formed due to melting driven by crustal thickening after continent-continent collision  
798 (Coffield et al., 1993; Bergman et al., 1996). This idea was largely influenced by the  
799 interpretation of: (1) widespread thrusting during the Oligocene and Mio-Pliocene;  
800 and (2) isotopic measurements from the Mio-Pliocene granitoids recording inherited  
801 Paleozoic ages (Bergman et al., 1996).

802

803 Our work has raised several questions about these earlier interpretations. For instance  
804 there is little evidence for widespread thrusting in the Oligocene and Mio-Pliocene in  
805 the Latimojong region. Most of the contacts that we observed were sub-vertical strike-  
806 slip fault zones (as well as mylonites in granite), no definite thrusts were found.

807

808 The same can be said about the inference of post-collision melting based on Paleozoic  
809 age data obtained from various isotopic measurements of the granitoids (e.g. Bergman  
810 et al., 1996). These simply show that the granites partially melted sedimentary rocks  
811 composed of Paleozoic detritus. These data alone do not indicate an episode of  
812 collision or thrusting occurred.

813

814 We interpret the medium- to high-grade metamorphic rocks exposed in the



815 Latimojong Mountains (the Latimojong Metamorphic Complex) to be equivalent to  
816 similar lithologies observed in Barru and Bantimala (e.g. Wakita et al., 1996;  
817 Parkinson et al., 1998). These rocks represent the basement, and younger sequences  
818 were deposited above an unconformity that developed during the Cretaceous.

819

820 It seems that Upper Cretaceous and Paleocene rocks have been removed from the  
821 stratigraphic record in the Latimojong region, with widespread development of a  
822 regional angular unconformity that is found at the top of Upper Cretaceous units (van  
823 Leeuwen and Muhardjo, 2005), possibly due to uplift associated with a short lived  
824 phase of subduction during the Paleocene (Hall, 2012). Continental and shallow water  
825 sedimentation commenced again during the Eocene and continued into the Oligocene  
826 (e.g. Toraja Group). This was associated with rifting and was interspersed with  
827 periods of arc and backarc volcanism (e.g. Lamasi Complex). However, the collision  
828 of the Sula Spur with Sulawesi's North Arm in the Early Miocene caused uplift and  
829 the development of another unconformity. Later there was a period of relative  
830 quiescence and growth of pinnacle and patch reefs (Makale Formation) during the  
831 Early to Middle Miocene. This was followed by a renewed phase of magmatism,  
832 related to crustal extension (Maulana et al., 2016) and/or flux-melting of the mantle  
833 wedge driven by subduction (i.e. the crustal extension could be driven by slab  
834 rollback and hinge migration). This produced the high K granitoids and volcanics  
835 during the Late Miocene to Pliocene (Palopo Granite / Enrekang Volcanic Series).  
836 Further uplift, alluvial fan deposition and strike slip faulting occurred later during the  
837 Pliocene to Pleistocene (e.g. Walanae Formation).

838

## 839 **10. Conclusion**

840 New biostratigraphic, geochronological and geochemical analyses have provided  
841 information about the tectonic history of the Latimojong region of South Sulawesi.  
842 This began with the development of an accretionary complex (the Latimojong  
843 Metamorphic Complex) that was assembled during the Cretaceous. These rocks were  
844 subsequently deformed and uplifted above sea level at some point before the Eocene.  
845 This may have been associated with the obduction of Eocene-Oligocene back-arc  
846 rocks (the Lamasi Complex). Deposition of clastic material recommenced during the  
847 Eocene, first in a terrestrial setting, which later evolved to reefs and near shore marine  
848 deposits (Toraja Formation). Subsequence phases of volcanism occurred during the

849 Miocene to Pliocene (Enrekang Volcanic Series/Palopo Pluton) and were  
850 contemporaneous with patch reef development (Makale Formation). Most of these  
851 sequences were then tectonically juxtaposed along strike-slip fault zones that  
852 developed due to transpressional forces associated opening of Bone Bay. This period  
853 of deformation probably also drove the uplift of the Latimojong region, which in turn  
854 led to alluvial deposits during the mid-Pliocene to present.

855

856 Our mapping of the region indicates substantial differences from earlier work. For  
857 instance, we found no clear evidence of thrusts between geological units. However,  
858 we did find evidence of brittle to ductile strike slip faults that were active between 6.3  
859 Ma and 5.0 Ma according to our geochronological work. We also found that the  
860 Latimojong Formation does not occur anywhere near the Latimojong region. Both of  
861 these points will help to resolve issues associated with correlating lithostratigraphic  
862 units across different parts of Sulawesi and in developing more accurate tectonic  
863 models of the region.

864

865

#### 866 **Acknowledgements**

867 This work was sponsored by a consortium of energy companies who fund the  
868 Southeast Asia Research Group (SEARG) and we are grateful for this support. We  
869 thank Kevin D'Souza for photographing the macroscopic detail of hand-specimens,  
870 Ega Nugraha and Karen Oud for assistance collecting and preparing samples, as well  
871 as Shane Paxton and Bin Fu for mineral separation and geochronology sample  
872 preparation. We would also like to thank Theo van Leeuwen for his thorough review  
873 of this manuscript.

874

875

876 **References**

- 877 Ascaria, N.A., 1997. Carbonate facies development and sedimentary evolution of the  
878 Miocene Tacipi Formation, South Sulawesi, Indonesia. PhD Thesis. University of  
879 London, 397 p.
- 880 Audley-Charles, M.G., 1974. Sulawesi. In: Spencer, A.M. (Ed.), *Mesozoic-Cenozoic*  
881 *Orogenic Belts*, Geological Society of London Special Publication, 4, 365–378.
- 882 Baharuddin, Harahap, B.H., 2000. Tinjauan kembali kerangka stratigrafi dan tektonik  
883 daerah Palopo, Sulawesi Selatan. *J. Geol. Sumberdaya Min.* 10, 24–38.
- 884 Bergman, S.C., Coffield, D.Q., Talbot, J.P., Garrard, R.J., 1996. Tertiary tectonic and  
885 magmatic evolution of Western Sulawesi and the Makassar Strait, Indonesia:  
886 Evidence for a Miocene continent-continent collision. In: Hall, R., Blundell, D.J.  
887 (Eds.), *Tectonic Evolution of SE Asia*, Geological Society of London Special  
888 Publication, 106, 391–430.
- 889 Berry, R.F., Grady, A.E., 1987. Mesoscopic structures produced by Plio-Pleistocene  
890 wrench faulting in South Sulawesi, Indonesia. *Journal of Structural Geology* 9,  
891 563–571.
- 892 Black, L., Kamo, S., Allen, C., Davis, D., Aleinikoff, J., Valley, J., Mundil, R.,  
893 Campbell, I., Korsch, R., Williams, I.S., 2004. Improved  $^{206}\text{Pb}/^{238}\text{U}$  microprobe  
894 geochronology by the monitoring of a trace-element-related matrix effect;  
895 SHRIMP, ID-TIMS, ELA-ICP-MS and oxygen isotope documentation for a  
896 series of zircon standards. *Chemical Geology* 205, 115–140.
- 897 BouDagher-Fadel, M.K., 2008. *Evolution and Geological Significance of Larger*  
898 *Benthic Foraminifera*. *Developments in Palaeontology and Stratigraphy*. Elsevier,  
899 Amsterdam.
- 900 Boudagher-Fadel, M.K., 2013. *Biostratigraphic and geological significance of*  
901 *planktonic foraminifera*, 2nd ed. University College London, London, United  
902 Kingdom.
- 903 Brouwer, H.A., 1934. *Geologische onderzoeken op het eiland Celebes*. Kolinien  
904 *Geologische-Mijnbouw Genootschap, Verhandelingen*. *Geologische Series* 10,  
905 39–218.
- 906 Calvert, S.J., 2000. The Cenozoic evolution of the Lariang and Karama basins,  
907 Sulawesi. *Indonesian Petroleum Association Proceedings 27th Annual*  
908 *Convention*, 505–511.

- 909 Calvert, S.J., Hall, R., 2007. Cenozoic evolution of the Lariang and Karama regions,  
910 North Makassar Basin, western Sulawesi, Indonesia. *Petroleum Geoscience* 13,  
911 353–368.
- 912 Camplin, D. J., Hall, R., 2014. Neogene history of Bone Gulf, Sulawesi, Indonesia.  
913 *Marine and Petroleum Geology* 57, 88–108.
- 914 Chamberlain, M., Seago, R., 1995. Geological Evaluation of the Lariang PSC area,  
915 South Sulawesi., Unpublished Report. Amoseas International.
- 916 Claoué-Long, J.C., Compston, W., Roberts, J., Fanning, C.M., 1995. Two  
917 Carboniferous Ages: a Comparison of SHRIMP Zircon Dating with Conventional  
918 Zircon Ages and  $^{40}\text{Ar}/^{39}\text{Ar}$  Analysis, in: Berggen, W.A., Kent, D.V., Aubry, M.P.,  
919 Hardenbol, J. (Eds.), *Geochronology Time Scales and Global Stratigraphic*  
920 *Correlation*, SEPM Special Publication, pp. 3–21.
- 921 Coffield, D.Q., Bergman, S.C., Garrard, R.A., Guritno, N., Robinson, N.M., Talbot,  
922 J., 1993. Tectonic and Stratigraphic Evolution of the Kalosi PSC Area and  
923 Associated Development of a Tertiary Petroleum System, South Sulawesi,  
924 Indonesia. *Proceedings of the Indonesian Petroleum Association 22nd Annual*  
925 *Convention*, 679–706.
- 926 Djuri and Sudjarmiko. 1974. Geologic map of the Majene and western part of the  
927 Palopo quadrangles, South Sulawesi (1:250,000). Geological Survey of Indonesia,  
928 Ministry of Mines, Bandung, Indonesia.
- 929 Djuri, Sudjarmiko, Bachri, S., Sukido. 1998. Geological map of the Majene and  
930 western part of the Palopo sheets, Sulawesi (1:250,000), 2<sup>nd</sup> Edition. Geological  
931 Research and Development Centre, Bandung, Indonesia.
- 932 Elburg, M., Foden, J., 1998. Temporal changes in arc magma geochemistry, northern  
933 Sulawesi, Indonesia. *Earth and Planetary Science Letters* 163, 381–398.
- 934 Elburg, M., Foden, J., 1999a. Sources for magmatism in Central Sulawesi:  
935 geochemical and Sr–Nd–Pb isotopic constraints. *Chemical Geology* 156, 67–93.
- 936 Elburg, M.A., Foden, J., 1999b. Geochemical response to varying tectonic settings:  
937 An example from southern Sulawesi (Indonesia). *Geochimica Cosmochimica*  
938 *Acta* 63, 1155–1172.
- 939 Elburg, M., van Leeuwen, T., Foden, J., Muhandjo, 2003. Spatial and temporal  
940 isotopic domains of contrasting igneous suites in Western and Northern Sulawesi,  
941 Indonesia. *Chemical Geology* 199, 243–276.

- 942 Endaharto, M., 2000. Studi stratigrafi kaitannya dengan perkembangan struktur  
943 geologi di Kawasan Latimojong, lengan Barat Sulawesi. *Jurnal Geologi dan*  
944 *Sumberdaya Mineral* 10, 107 p.
- 945 Frost, B.R., Barnes, C.G., Collins, W.J., Arculus, R.J., Ellis, D.J., Frost, C.D., 2001.  
946 A geochemical classification for granitic rocks. *Journal of Petrology* 42, 2033–  
947 2048.
- 948 Frost, B.R., Frost, C.D., 2008. A geochemical classification for feldspathic igneous  
949 rocks. *Journal of Petrology* 49, 1955–1969.
- 950 Gradstein, F.M., Ogg, J.G., Schmitz, M.D., Ogg, G.M., 2012. *The Geological Time*  
951 *Scale 2012*, 1st ed. Elsevier.
- 952 Grainge, A.M., Davies, K.G., 1985. Reef exploration in the east Sengkang Basin,  
953 Sulawesi, Indonesia. *Marine and Petroleum Geology* 2, 142–155.
- 954 Hadiwijoyo, S., Sukarna, D. & Sutisna, K. 1993. *Geology of the Pasangkayu*  
955 *Quadrangle, Sulawesi. (Quadrangle 2014) Scale 1:250,000*. Geological Research  
956 and Development Centre, Bandung, Indonesia.
- 957 Hall, R., 1996. Reconstructing Cenozoic SE Asia. In: Hall, R., Blundell, D.J. (Eds.),  
958 *Tectonic Evolution of SE Asia*, Geological Society London Special Publication  
959 106, 153–184.
- 960 Hall, R., 2002. Cenozoic geological and plate tectonic evolution of SE Asia and the  
961 SW Pacific: computer-based reconstructions, model and animations. *Journal of*  
962 *Asian Earth Sciences* 20, 353–431.
- 963 Hall, R., 2012. Late Jurassic–Cenozoic reconstructions of the Indonesian region and  
964 the Indian Ocean. *Tectonophysics* 570-571, 1–41.
- 965 Hamilton, W.B., 1979. *Tectonics of the Indonesian region*. USGS Professional Paper  
966 1078, 345 pp.
- 967 Hasan, K., 1991. The Upper Cretaceous Flysch Succession of the Balangbaru  
968 Formation, Southwest-Sulawesi. *Proceedings of the Indonesian Petroleum*  
969 *Association 20th Annual Convention*, 183–208.
- 970 Hennig, J., Hall, R., Armstrong, R.A. 2016. U-Pb zircon geochronology of rocks from  
971 west Central Sulawesi, Indonesia: Extension-related metamorphism and  
972 magmatism during the early stages of mountain building. *Gondwana Research* 32,  
973 41–63. doi:10.1016/j.gr.2014.12.012
- 974 Jaya, A., Nishikawa, O., 2013. Paleostress reconstruction from calcite twin and fault-  
975 slip data using the multiple inverse method in the East Walanae fault zone:

- 976 Implications for the Neogene contraction in South Sulawesi, Indonesia. *Journal of*  
977 *Structural Geology* 55, 34–49.
- 978 Katili, J.A., 1970. Large transcurrent faults in Southeast Asia with special reference to  
979 Indonesia. *Geologische Rundschau* 59, 581–600.
- 980 Katili, J.A., 1978. Past and present geotectonic position of Sulawesi, Indonesia.  
981 *Tectonophysics* 45, 289–322.
- 982 Ludwig, K.R., 2003. *Isoplot 3.00: A Geochronological Toolkit for Microsoft Excel*.  
983 *Berkeley Geochronological Centre Special Publication* 4, 70 pp.
- 984 Ludwig, K.R., 2009. *SQUID 2, A User's Manual*. *Berkeley Geochronological Centre*  
985 *Special Publication* 5, 110 pp.
- 986 Maryanto, S. 2002. Stratigrafi tersier daerah Toraja, 31<sup>st</sup> Annual Convention of  
987 Indonesian Association of Geologists, 734-768.
- 988 Maulana, A., Ellis, D.J., Christy, A.G., 2010. Petrology, geochemistry and tectonic  
989 evolution of the South Sulawesi basement rocks. *Proceedings of the Indonesian*  
990 *Petroleum Association 34th Annual Convention*, IPA10-G-192 1–26.
- 991 Maulana, A., Imai, A., van Leeuwen, T., Watanabe, K., Yonezu, K., Nakano, T.,  
992 Boyce, A., Page, L., Schersten, A. 2016. Origin and geodynamic setting of Late  
993 Cenozoic granitoids in Sulawesi, Indonesia. *Journal of Asian Earth Sciences* 124,  
994 102-125.
- 995 O'Dogherty, L., 2009. Inventory of Mesozoic radiolarian species (1867-2008).  
996 *Geodiversitas* 31, 371–503. doi:<http://dx.doi.org/10.5252/g2009n2a6>
- 997 Parkinson, C., 1998. Emplacement of the East Sulawesi Ophiolite: evidence from  
998 subophiolite metamorphic rocks *Journal of Asian Earth Sciences* 16, 13–28.
- 999 Parkinson, C.D., Miyazaki, K., Wakita, K., Barber, A.J., Carswell, D.A., 1998. An  
1000 overview and tectonic synthesis of the pre-Tertiary very- high-pressure  
1001 metamorphic and associated rocks of Java, Sulawesi and Kalimantan, Indonesia.  
1002 *Island Arc* 7, 184–200.
- 1003 Polvé, M., Maury, R.C., Bellon, H., Rangin, C., Priadi, B., Yuwono, S., Joron, J.L.,  
1004 Atmadja, R.S., 1997. Magmatic evolution of Sulawesi (Indonesia): constraints on  
1005 the Cenozoic geodynamic history of the Sundaland active margin. *Tectonophysics*  
1006 272, 69–92.
- 1007 Priadi, B., Polvé, M., Maury, R.C., Bellon, H., Soeria-Atmadja, R., Joron, J.L.,  
1008 Cotten, J., 1994. Tertiary and Quaternary magmatism in Central Sulawesi:

- 1009       chronological and petrological constraints. *Journal of Southeast Asian Earth*  
1010       *Sciences* 9, 81–93.
- 1011   Querubin, C. D., Walters, S. 2012. Geology and mineralization of Awak Mas: A  
1012       sedimentary hosted gold deposit, South Sulawesi, Indonesia. *Majalah Geologi*  
1013       *Indonesia* 27(2), 69-85.
- 1014   Ratman, N., Atmawinata, S., 1993. Geology of the Mamuju Quadrangle, Sulawesi.  
1015       Scale 1:250,000. Geological Survey of Indonesia, Directorate of Mineral  
1016       Resources, Geological Research and Development Centre, Bandung.
- 1017   Reijzer, J., 1920, Geologische aanteekeningen betreffende de Zuidelijke Toraja-  
1018       landen, verzameld uit de verslagen der mijnbouwkundige onderzoekingen in  
1019       Midden-Celebes. *Jaarboek van het Mijnwezen in Nederlandsch Oost-Indië* 47  
1020       (1918), deel 1 Verhandelingen, p. 154–209.
- 1021   Silver, E.A., McCaffrey, R., Joyodiwiryo, Y., Stevens, S., 1983a. Ophiolite  
1022       emplacement by collision between the Sula Platform and the Sulawesi island arc,  
1023       Indonesia. *Journal of Geophysical Research* 88, 9419–9435.
- 1024   Silver, E.A., McCaffrey, R., Smith, R.B., 1983b. Collision, rotation, and the initiation  
1025       of subduction in the evolution of Sulawesi, Indonesia. *Journal of Geophysical*  
1026       *Research*. 88, 9407–9418.
- 1027   Simandjuntak, T.O., Rusmana, E., Suroño, Supandjono, J.B., 1991. Geology of the  
1028       Malili Quandrangle, Sulawesi. Scale 1:250,000. Geological Research and  
1029       Development Centre, Department of Mines and Energy, Bandung, Indonesia.
- 1030   Simandjuntak, T.O., Suroño, Sukido, 1994. Geology of the Kolaka Sheet, Sulawesi  
1031       (Quadrangles 2111, 2210, 2211), Scale 1:250,000, Geological Research and  
1032       Development Centre, Bandung.
- 1033   Spakman, W., Hall, R. 2010. Surface deformation and slab-mantle interaction during  
1034       Banda arc subduction rollback. *Nature Geoscience* 3, 562-566.
- 1035   Spencer, J. E., 2010. Structural analysis of three extensional detachment faults with  
1036       data from the 2000 Space-Shuttle Radar Topography Mission. *GSA Today* 20, 4–  
1037       10.
- 1038   Spencer, J.E., 2011. Gently dipping normal faults identified with Space Shuttle radar  
1039       topography data in central Sulawesi, Indonesia, and some implications for fault  
1040       mechanics. *Earth and Planetary Science Letters* 308, 267–276.

- 1041 Steiger, R.H., Jäger, E., 1977. Subcommittee on geochronology: convention on the  
1042 use of decay constants in geo- and cosmochronology. *Earth and Planetary Science*  
1043 *Letters* 36, 359–362.
- 1044 Sukamto, R., 1975. Geological map of the Ujung Pandang Sheet, Scale 1:1,000,000.  
1045 Geological Survey of Indonesia, Bandung.
- 1046 Sukamto, R., 1982. Geological map of Pangkajene and Watampone Quadrangles,  
1047 Scale 1:250,000. Indonesian Geological Research and Development Centre,  
1048 Bandung.
- 1049 Sukamto, R., Simandjuntak, T.O., 1983. Tectonic relationship between geologic  
1050 provinces of Western Sulawesi, Eastern Sulawesi and Banggai-Sula in the light of  
1051 sedimentological aspects. *Bulletin of the Geological Research and Development*  
1052 *Centre* 7, 1–12.
- 1053 Surono, 1994. Stratigraphy of the southeast Sulawesi continental terrane, Eastern  
1054 Indonesia. *Journal of Geology and Mineral Resources* 4, 4–11.
- 1055 van Leeuwen, T.M., 1981. The geology of southwest Sulawesi with special reference  
1056 to the Biru area. In: Barber, A.J., Wiryosujono, S. (Eds.), *The Geology and*  
1057 *Tectonics of Eastern Indonesia*, Geological Research and Development Centre,  
1058 Bandung, Special Publication, 2, 277–304.
- 1059 van Leeuwen, T.M., Muhardjo, 2005. Stratigraphy and tectonic setting of the  
1060 Cretaceous and Paleogene volcanic-sedimentary successions in northwest  
1061 Sulawesi, Indonesia: implications for the Cenozoic evolution of Western and  
1062 Northern Sulawesi. *Journal of Asian Earth Sciences* 25, 481–511.
- 1063 van Leeuwen, T.M., Pieters, P. E., 2011. Mineral Deposits of Sulawesi. Proceedings  
1064 of the Sulawesi Mineral Resources 2011 Seminar, MGEI-IAGI, 28-29 November,  
1065 2011, Manado, North Sulawesi, Indonesia, pp. 130, doi:10.13140/2.1.3843.2322
- 1066 van Leeuwen, T., Allen, C.M., Kadarusman, A., Elburg, M., Michael Palin, J.,  
1067 Muhardjo, Suwijanto, 2007. Petrologic, isotopic, and radiometric age constraints  
1068 on the origin and tectonic history of the Malino Metamorphic Complex, NW  
1069 Sulawesi, Indonesia. *Journal of Asian Earth Sciences* 29, 751–777.
- 1070 van Leeuwen, T.M., Susanto, E.S., Maryanto, S., Hadiwisastra, S., Sudijono,  
1071 Muhardjo, Prihardjo, 2010. Tectonostratigraphic evolution of Cenozoic marginal  
1072 basin and continental margin successions in the Bone Mountains, Southwest  
1073 Sulawesi, Indonesia. *Journal of Asian Earth Sciences* 38, 233-254.



- 1074 van Leeuwen, T., Allen, C.M., Elburg, M., Massonne, H.-J., Palin, J.M., Hennig, J.,  
1075 2016. The Palu Metamorphic Complex, NW Sulawesi, Indonesia: Origin and  
1076 evolution of a young metamorphic terrane with links to Gondwana and  
1077 Sundaland. *Journal of Asian Earth Sciences* 115, 133–152.
- 1078 Wakita, K., Sopaheluwakan, J., Miyazaki, K., Zulkarnain, I., Munasri, 1996. Tectonic  
1079 evolution of the Bantimala Complex, South Sulawesi, Indonesia. In: Hall, R.,  
1080 Blundell, D.J. (Eds.), *Tectonic Evolution of SE Asia*, Geological Society of  
1081 London Special Publication, 106, 353–364.
- 1082 Watkinson, I.M., Hall, R., Ferdian, F., 2011. Tectonic re-interpretation of the  
1083 Banggai-Sula–Molucca Sea margin, Indonesia. In: Hall, R., Cottam, M.A.,  
1084 Wilson, M.E.J. (Eds.), *The SE Asian Gateway: History and Tectonics of the*  
1085 *Australia-Asia collision*, Geological Society of London Special Publication, 355,  
1086 203–224.
- 1087 White, L.T., Ireland, T.R., 2012. High-uranium matrix effect in zircon and its  
1088 implications for SHRIMP U–Pb age determinations. *Chemical Geology* 306-307,  
1089 78–91.
- 1090 White, L.T., Hall, R., Armstrong, R.A., 2014. The age of undeformed dacite  
1091 intrusions within the Kolaka Fault Zone, SE Sulawesi, Indonesia. *Journal of*  
1092 *Asian Earth Sciences* 94, 105–112.
- 1093 Williams, I.S., 1998. U-Th-Pb Geochronology by Ion Microprobe, in: McKibben,  
1094 M.A., Shanks, W.C., III, Ridley, W.I. (Eds.), *Applications of microanalytical*  
1095 *techniques to understanding mineralizing processes*. *Reviews in Economic*  
1096 *Geology* 7, 1–35.
- 1097 Wilson, M.E.J., Bosence, D.W.J., 1996. The Tertiary Evolution of South Sulawesi: A  
1098 Record in Redeposited Carbonates of the Tonasa Limestone Formation. In: Hall,  
1099 R., Blundell, D.J. (Eds.), *Tectonic Evolution of SE Asia*, Geological Society of  
1100 London Special Publication, 106, 365–389.
- 1101 Yuwono, Y.S., Maury, R.C., Soeria-Atmadja, R., Bellon, H. 1988. Tertiary and  
1102 Quaternary geodynamic evolution of South Sulawesi: constraints from the study  
1103 of volcanic units. *Geologi Indonesia, Jakarta* 13(1), 32–48.
- 1104  
1105  
1106  
1107

1108 **Table Captions**

1109 *Table 1. Summary of the sample locations, lithologies and which samples were*  
1110 *selected for geochemical and U-Pb dating. The samples have been grouped according*  
1111 *to their petrology, proposed geological unit and their age (from youngest to oldest).*

1112

1113

1114 **Figure Captions**

1115 *Figure 1. Map showing the location of the geological terranes and major faults of*  
1116 *Sulawesi. The location of the Latimojong region and the focus of this study is shown*  
1117 *with a black box (adapted from White et al., 2014).*

1118

1119 *Figure 2. Geological map of the study area showing the location of major geological*  
1120 *units, interpreted structures as well as the location of samples and geographic*  
1121 *locations discussed in the text. All of the geological boundaries represent*  
1122 *interpreted, as contacts were not observed in the field. The ages reported on the*  
1123 *map, represent those obtained in this study.*

1124

1125 *Figure 3. Field photos of different units of the Lamasi Volcanics. These include (a-b)*  
1126 *pillow basalts, often with altered glass and interstitial chert; (c) vesicular and non-*  
1127 *vesicular basalt dykes, (d) gabbro, occasionally cross-cut by 1-10cm pegmatite veins*  
1128 *and dykes, and: (e) serpentinite or altered basalt.*

1129

1130 *Figure 4. Field photographs of the (a) 'red-bed' shales of the Toraja Formation and*  
1131 *the well-bedded deposits of fluvial sandstones.*

1132

1133 *Figure 5. Field photograph of the karst landscape on the western side of the*  
1134 *Latimojong Mountains. These carbonates are part of the Makale Formation, which is*  
1135 *the stratigraphic equivalent of the Tonasa Limestone.*

1136

1137 *Figure 6. Field photographs of the Enrekang Volcanic Series at the outcrop scale as*  
1138 *well as in hand specimen. Ages each of these outcrops/samples were acquired using*  
1139 *SHRIMP U-Pb dating of zircon. (a-b) Shows a felsic dyke (sample K12-33B) cross-*  
1140 *cutting basement schists of the Latimojong Complex; (c-d) shows a boulder of*  
1141 *porphyritic dacite (K12-27) within the inferred north-western continuation of the*

1142 *Kolaka Fault Zone; (e-f) shows quarry workers extracting this dacite as well as the*  
1143 *grain-scale detail of dacite sample K12-21A/B.*

1144

1145 *Figure 7. Field photographs of the granodiorites of the Palopo Granite. These*  
1146 *granodiorites are (a-c) undeformed in parts, but are (d-e) mylonitised in other*  
1147 *outcrops. The granites also contain xenoliths and enclaves, some of which show*  
1148 *evidence of (b) mingling between the granite and restite. (d) These enclaves have also*  
1149 *been flattened/stretched parallel to the mylonitic fabric in places and were later*  
1150 *cross-cut by aplitic dykes. Sample K12-4B represents an undeformed granodiorite*  
1151 *collected from the same location as is shown in (b) and (c). Sample K12-6A/6B were*  
1152 *deformed samples collected from the sample location as is shown in (d). Sample K12-*  
1153 *35B is a deformed granodiorite collected from the same location as is shown in (e).*

1154

1155 *Figure 8. An example of (a) the well-bedded sandstones and conglomerate continental*  
1156 *deposits of the Walanae Formation, as well as (b) some of the leaf fossils found within*  
1157 *finer-grained units of this formation.*

1158

1159 *Figure 9. Field photographs of the “Bua Rhyolite” which cross-cuts basalts of the*  
1160 *Lamasi Volcanics.*

1161

1162 *Figure 10. Scanning electron microscopy of radiolarians that were extracted from a*  
1163 *sample of chert float collected west of the Latimojong Mountains. These were*  
1164 *identified as follows: 1. *Stichomitra* cf. *japonica* (Nakaseko & Nishimura); 2 *Xitus* cf.*  
1165 *clava* (Parona); 3. Gen. sp. indet.; 4. Gen. sp. indet.; 5. *Dictyomitra* sp.; 6.  
1166 *Dictyomitra* sp.; 7. *Thanarla* cf. *pulchra* (Squinabol); 8. *Dictyomitra* sp.; 9.  
1167 *Distylocapsa* sp.; 10. Gen. sp. indet.; 11. *Hiscocapsa* sp.; 12. Gen. sp. Indet.; 13. Gen.  
1168 *sp. indet.*

1169

1170 *Figure 11. Chronostratigraphic chart and corresponding biostratigraphic ages*  
1171 *obtained from the identification of foraminifera in the Toraja Formation, Makale*  
1172 *Formation and the Enrekang Volcanic Series.*

1173

1174 *Figure 12. Tera-Wasserburg Concordia diagrams of the U-Pb SHRIMP results for*  
1175 *each of the igneous samples that were dated in this study.*

1176

1177 *Figure 13. Relative frequency apparent age plots of U-Pb SHRIMP results for each of*  
1178 *the igneous samples that were dated in this study.*

1179

1180 *Figure 14. Various plots showing the geochemical data collected from the igneous*  
1181 *rock samples that were collected as part of this study. The distinctive chemical groups*  
1182 *correspond with different petrological characteristics as well as the crystallization*  
1183 *ages of these rocks.*

1184

1185 *Figure 15. Revised chronostratigraphic chart for the Latimojong Mountains region*  
1186 *that takes the results of this and previous studies into account.*

1187

### 1188 **Supplementary Files**

1189 *Interactive Map File: A KMZ file containing location data of observed lithologies at*  
1190 *various field sites across the Latimojong region.*

1191

1192 *Supp. Data File 1. Details of foraminifera identified for various samples from the*  
1193 *Latimojong region of Sulawesi.*

1194

1195 *Supp. Data File 2. Representative and age determining foraminifera from the (a-h)*  
1196 *Toraja Formation, (i) Makale Formation and (j) Enrekang Volcanic Series: (a)*  
1197 *Cycloclypeus eidae [Sample: K12-10]; (b) Lepidocyclina isolepidinoides [Sample:*  
1198 *K12-10]; (c) Globoquadrina sp. [Sample: K12-14]; (d) Asterocyclina sp., [Sample:*  
1199 *K12-17]; (e) Discocyclina dispansa [Sample: K12-17]; (f) Nummulites sp. [K12-17];*  
1200 *(g) Pellatispira sp. [Sample: K12-17]; (h) Dentoglobigerina altispira [Sample: K12-*  
1201 *15]; (i) Globoquadrina dehiscens [Sample: K12-20B]; (j) Globorotalia miocenica*  
1202 *[Sample K12-22B].*

1203

1204 *Supp. Data File 3. Results of SHRIMP U-Pb analyses of zircons for the various*  
1205 *igneous rocks that were dated as part of this study.*

1206

1207 *Supp. Data File 4. Major and trace element data collected from whole-rock XRF*  
1208 *analyses of the igneous samples that were investigated as part of this study.*

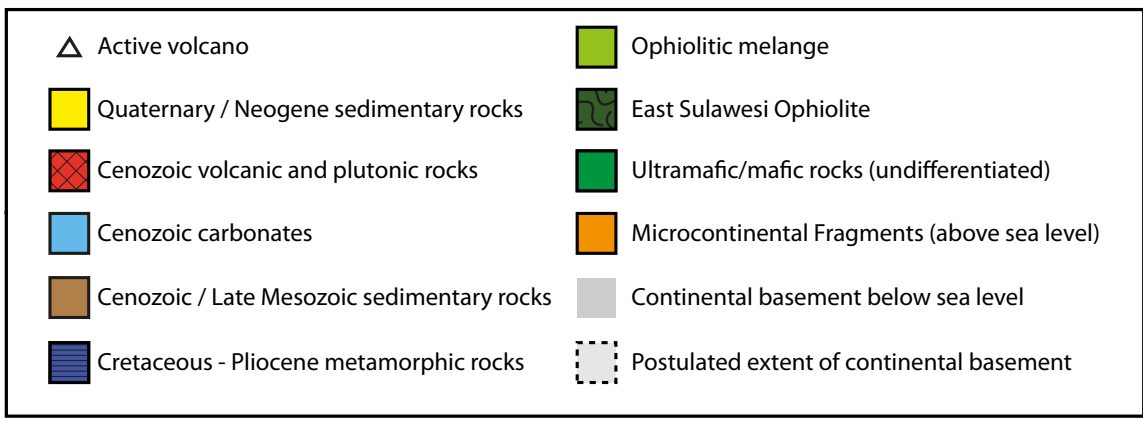
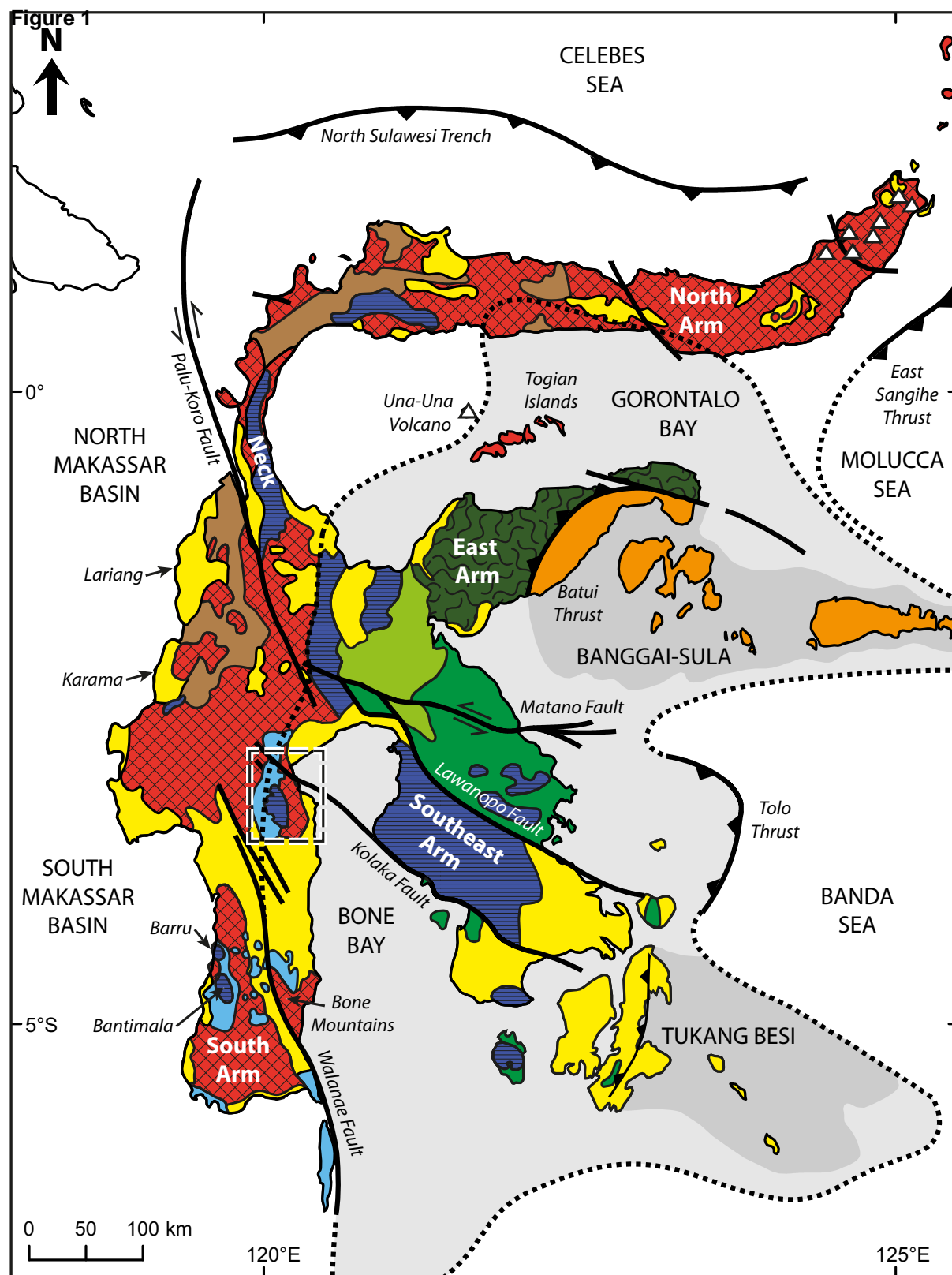


Figure 2

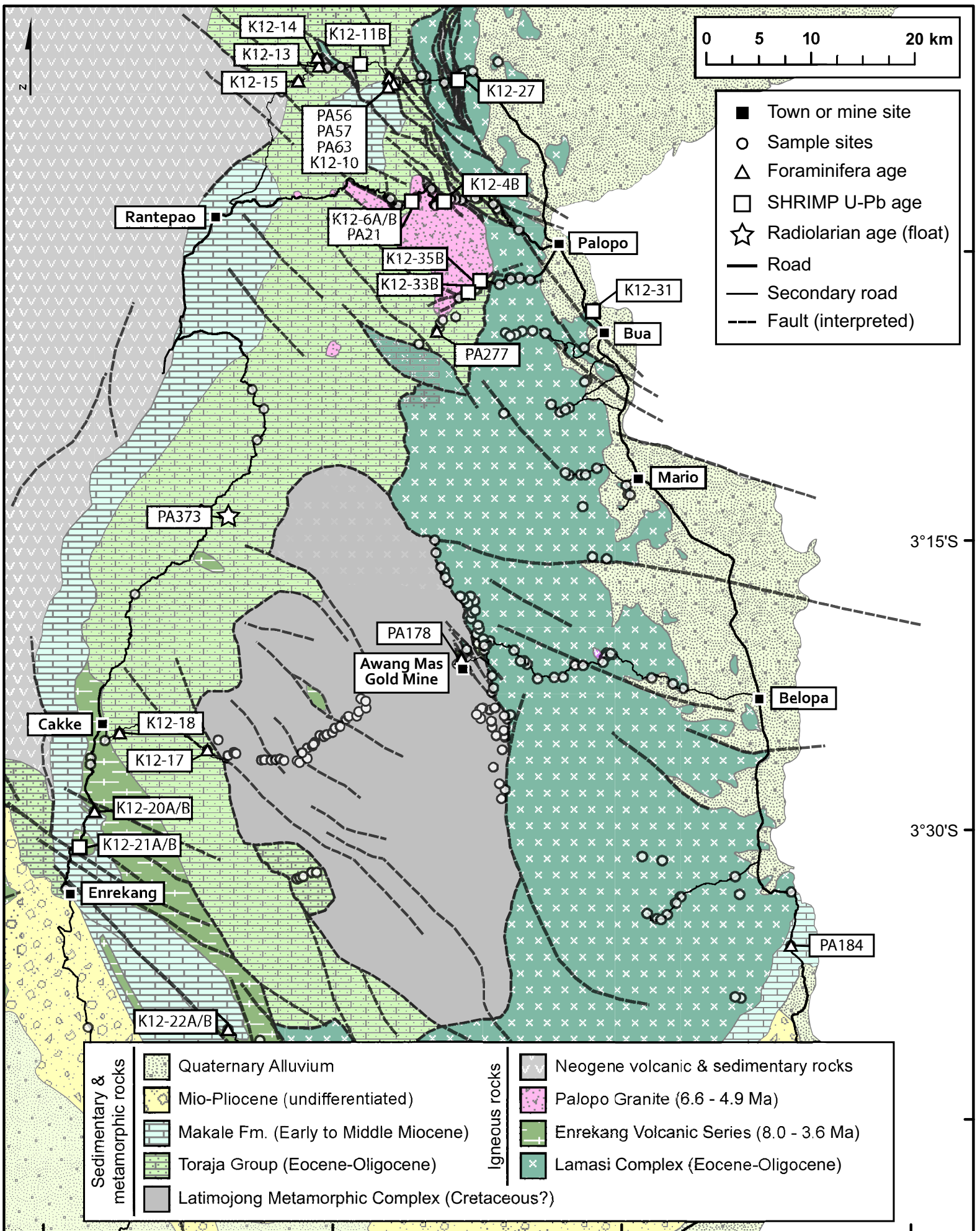




Figure 3  
[Click here to download high resolution image](#)

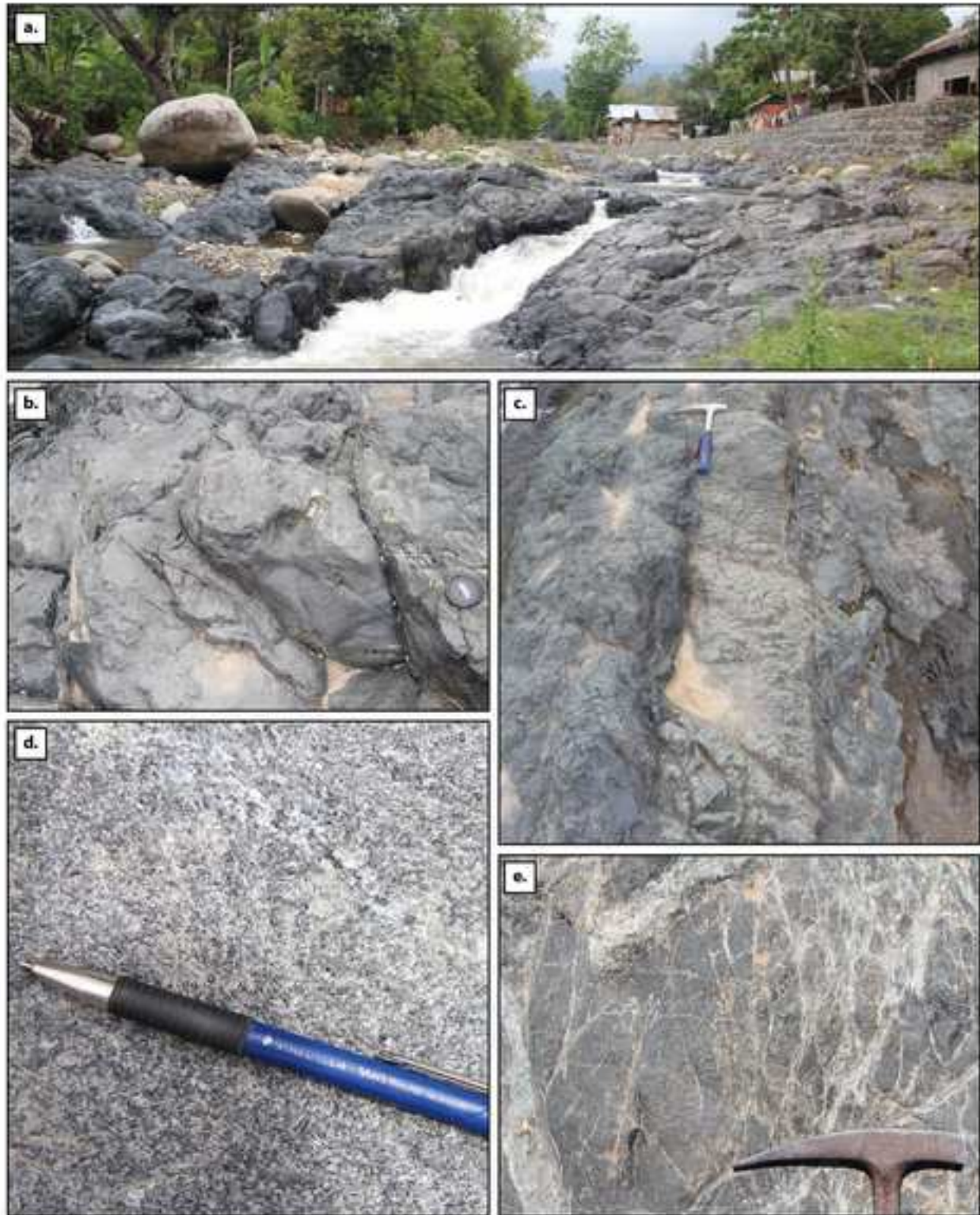


Figure 4

[Click here to download high resolution image](#)





Figure 5

[Click here to download high resolution image](#)



Figure 6  
[Click here to download high resolution image](#)

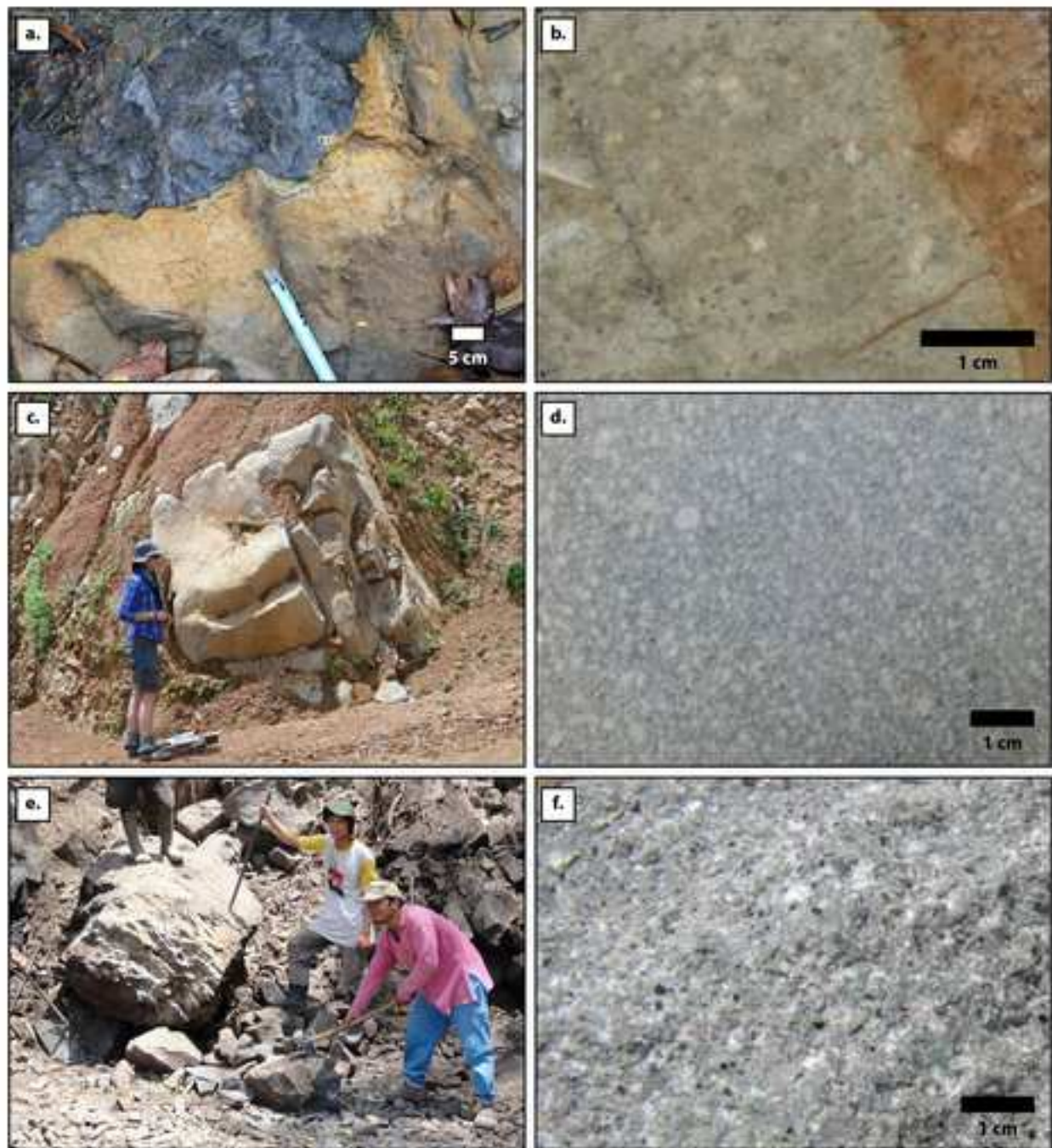




Figure 7  
[Click here to download high resolution image](#)



Figure 8  
[Click here to download high resolution image](#)





Figure 9

[Click here to download high resolution image](#)

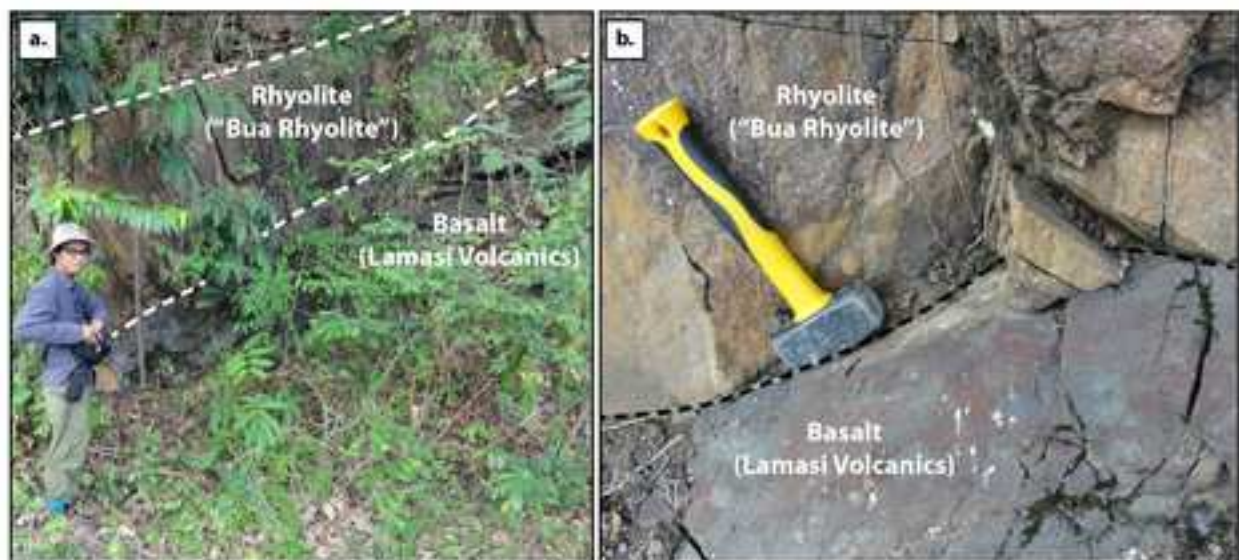


Figure 10  
[Click here to download high resolution image](#)

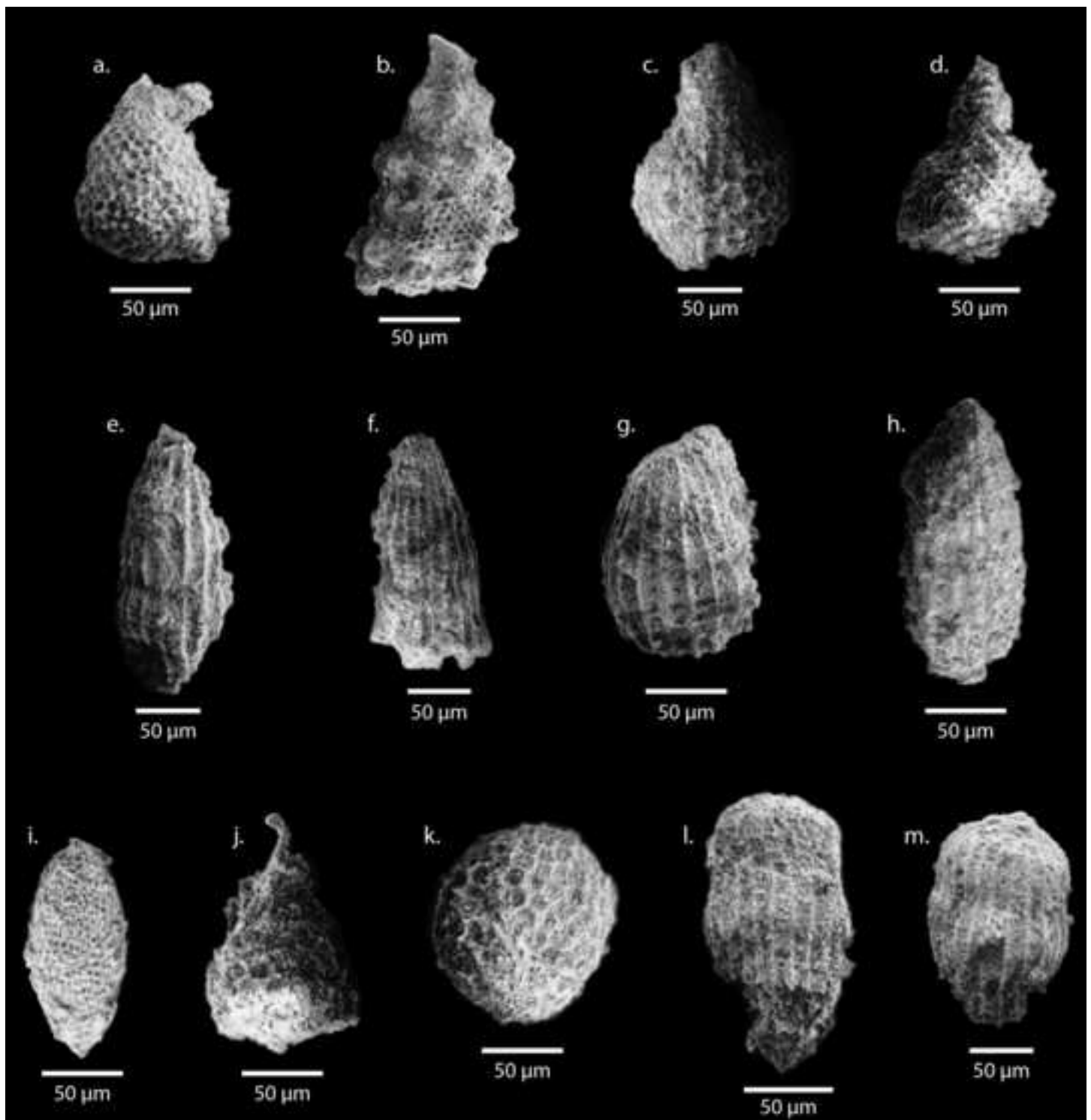
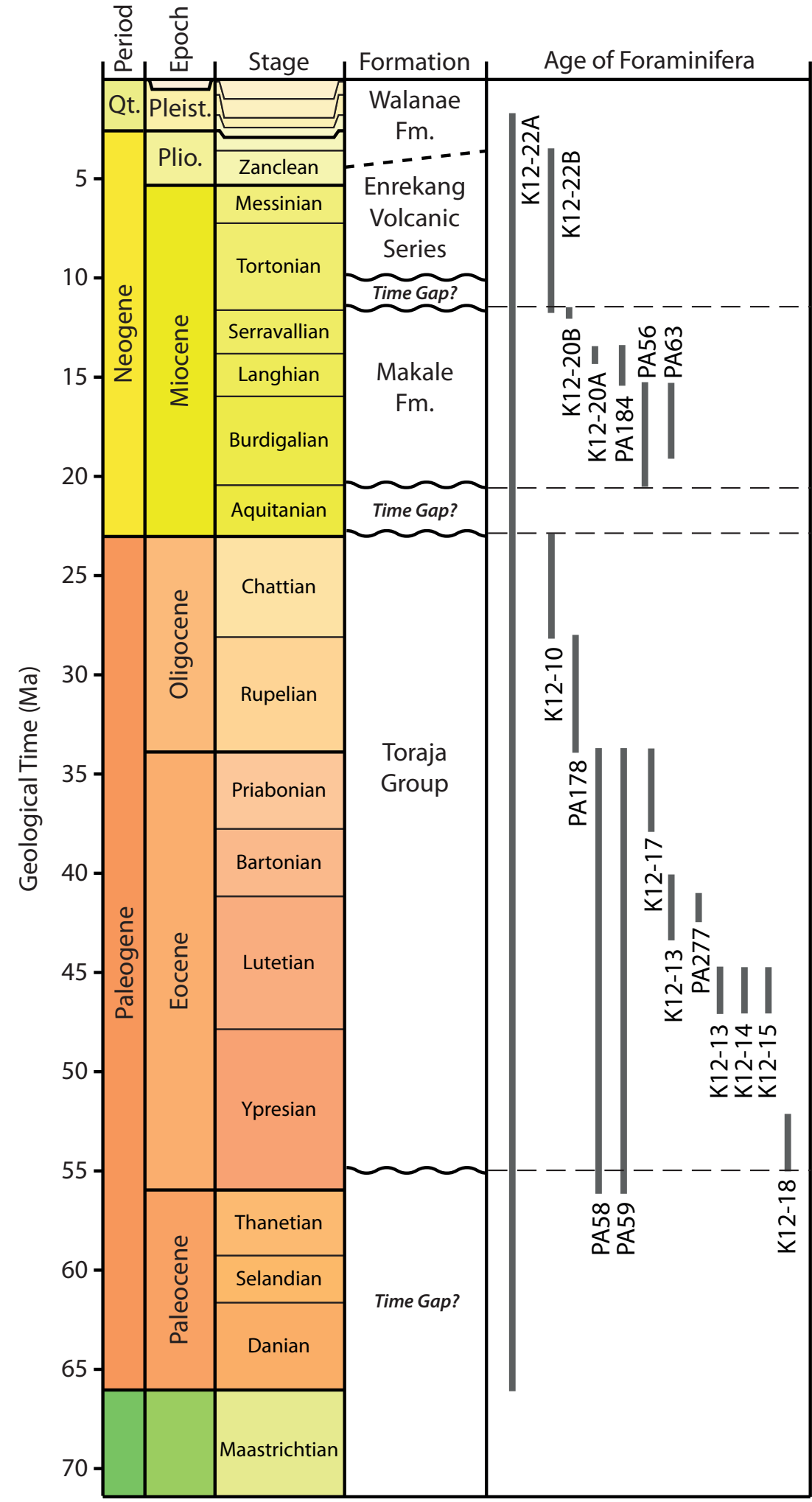
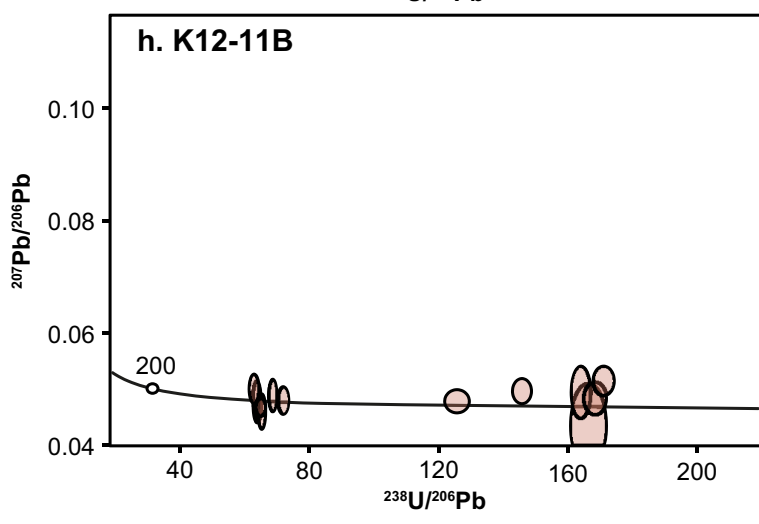
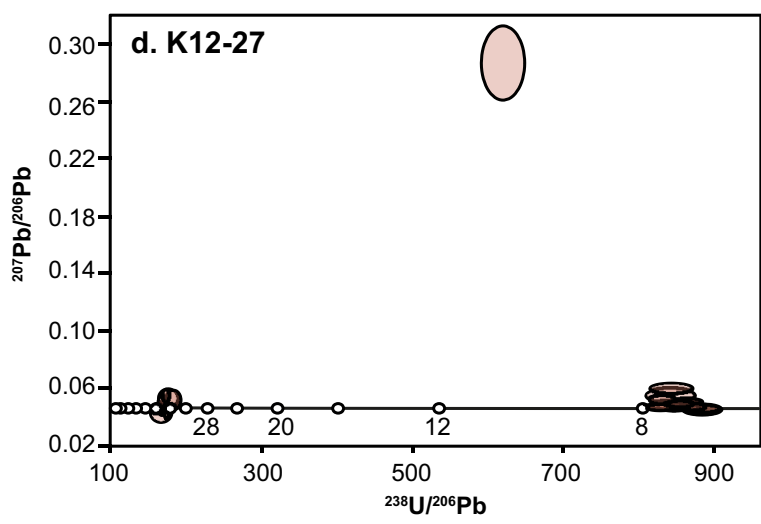
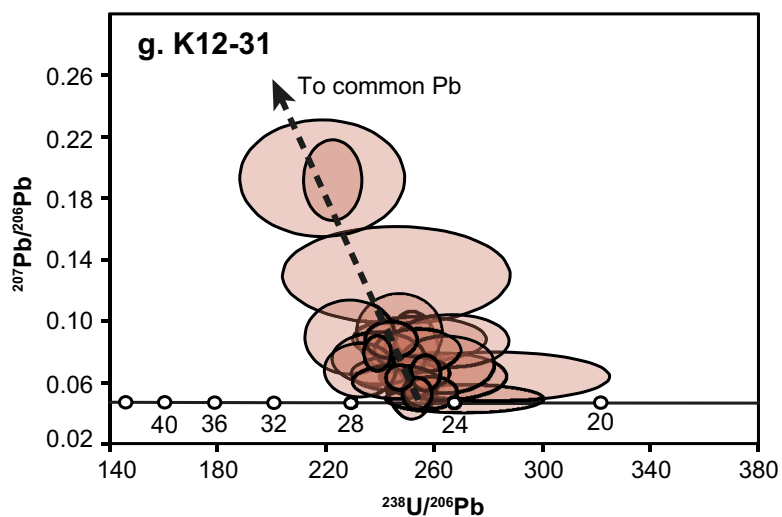
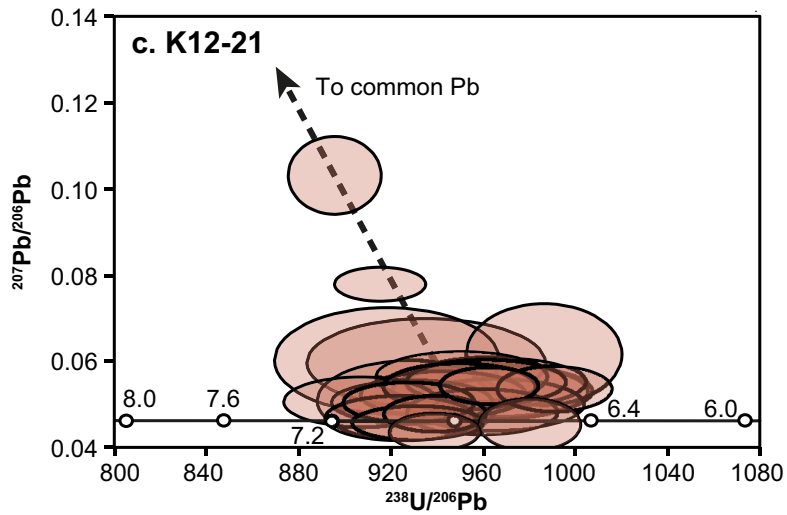
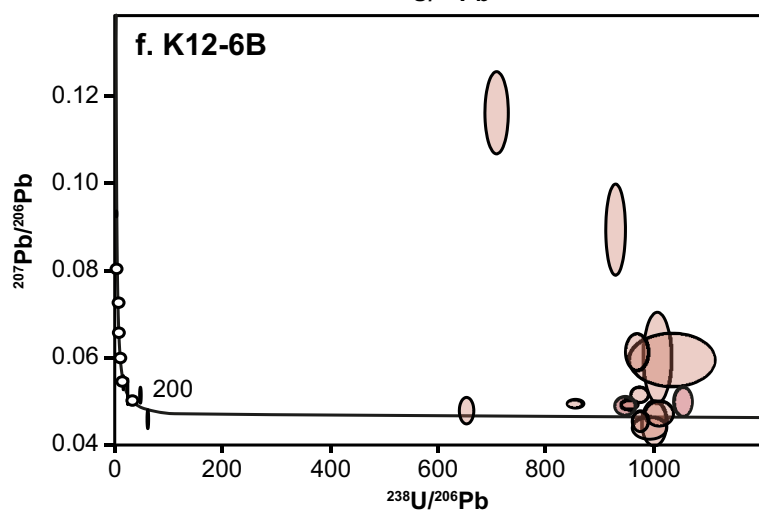
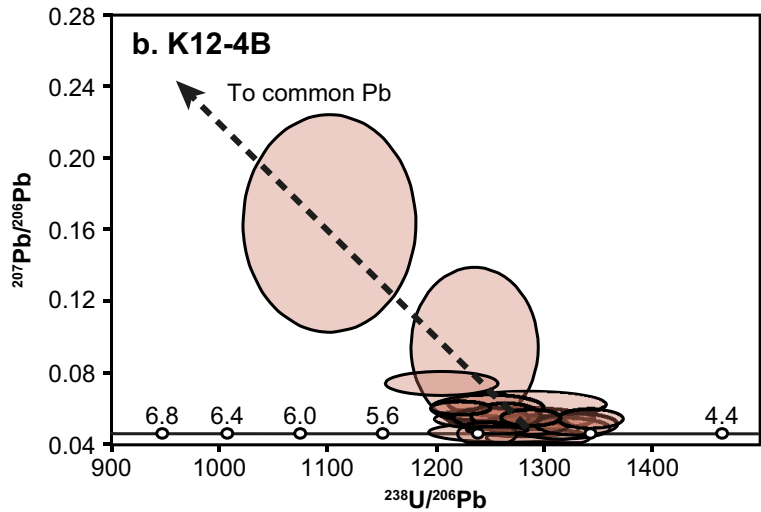
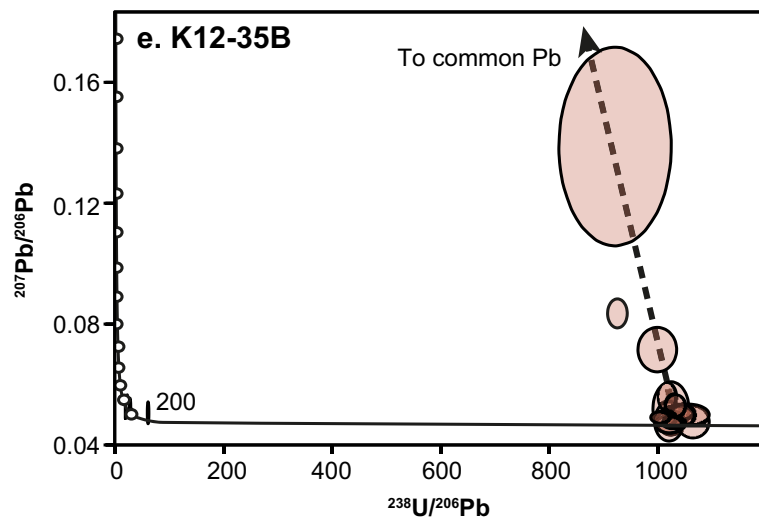
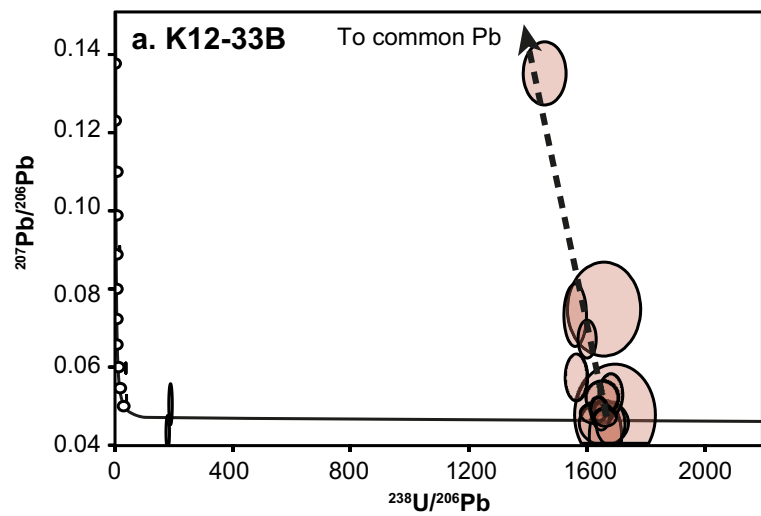
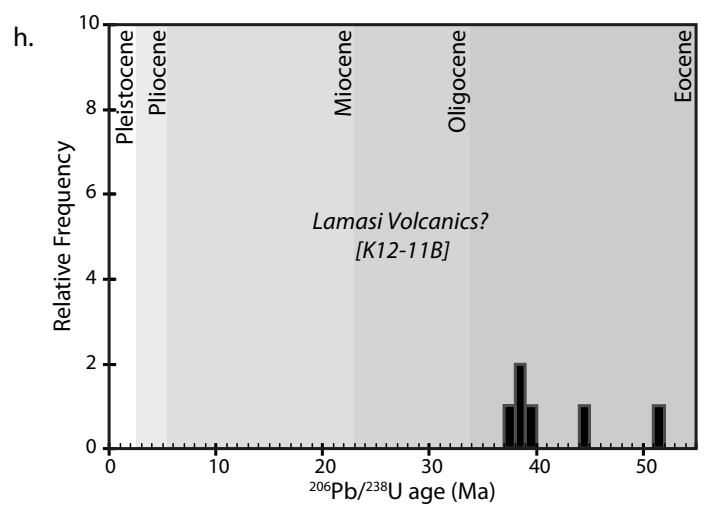
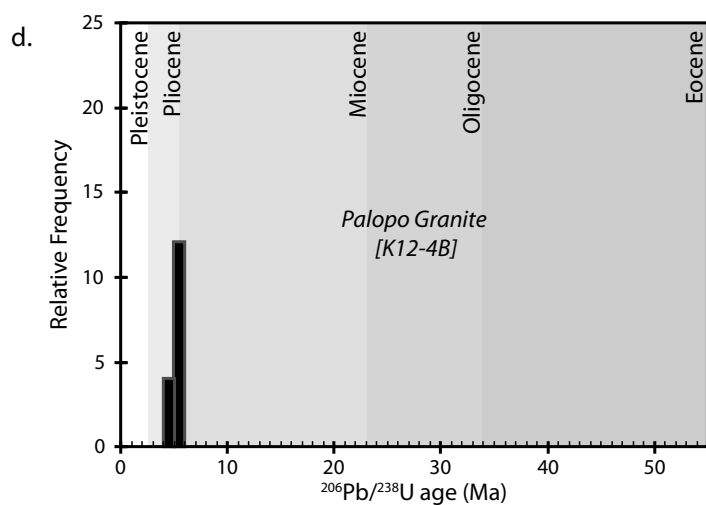
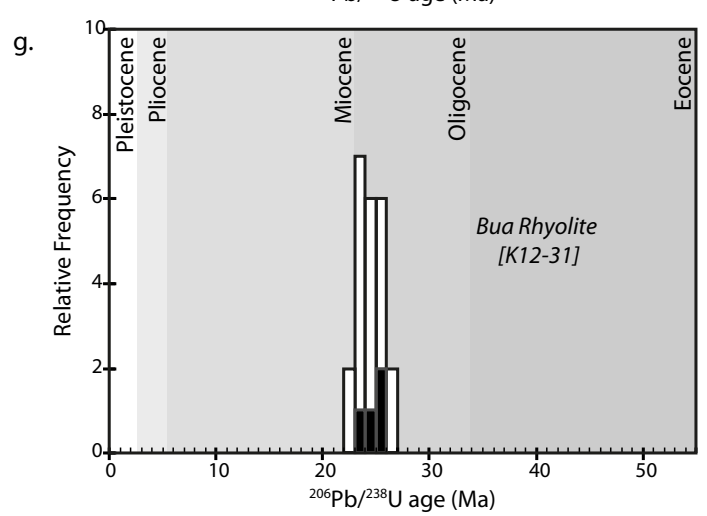
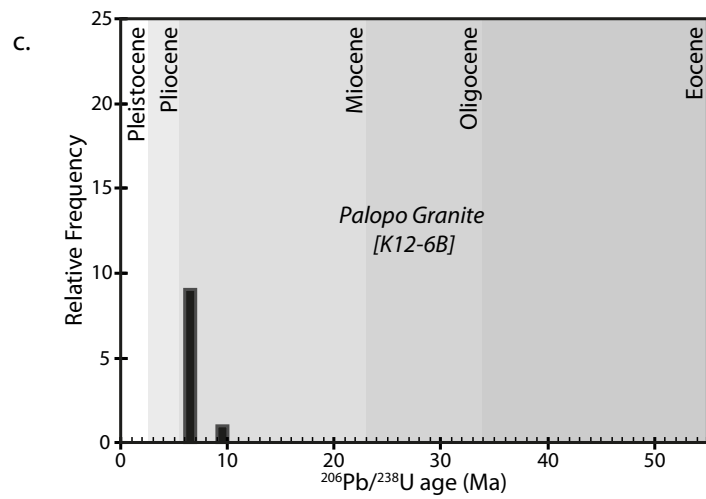
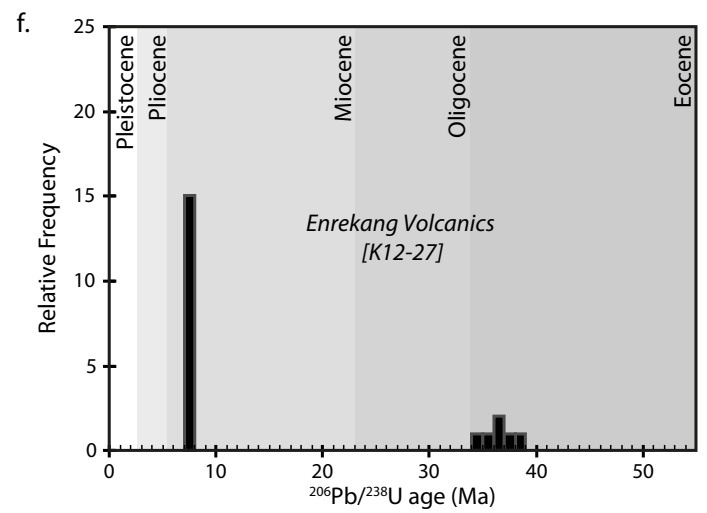
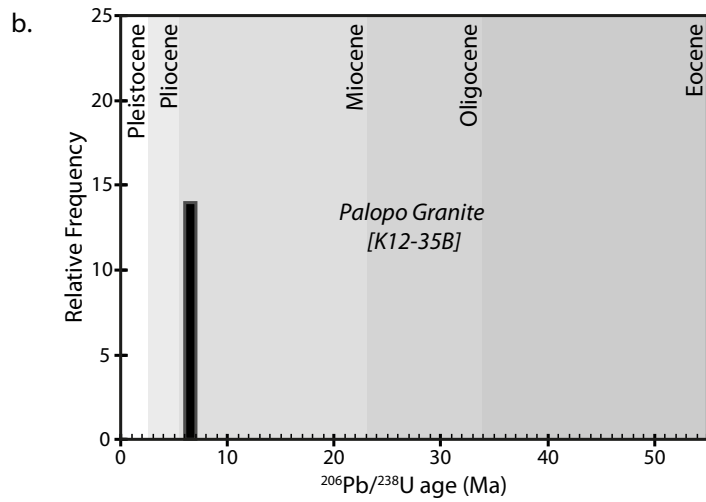
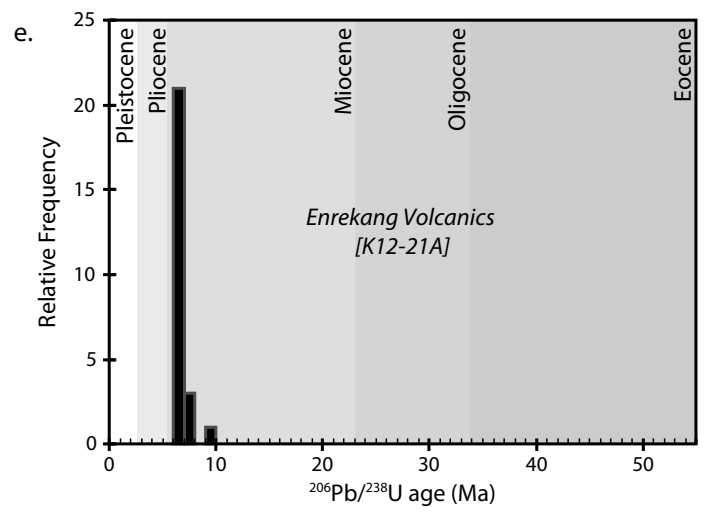
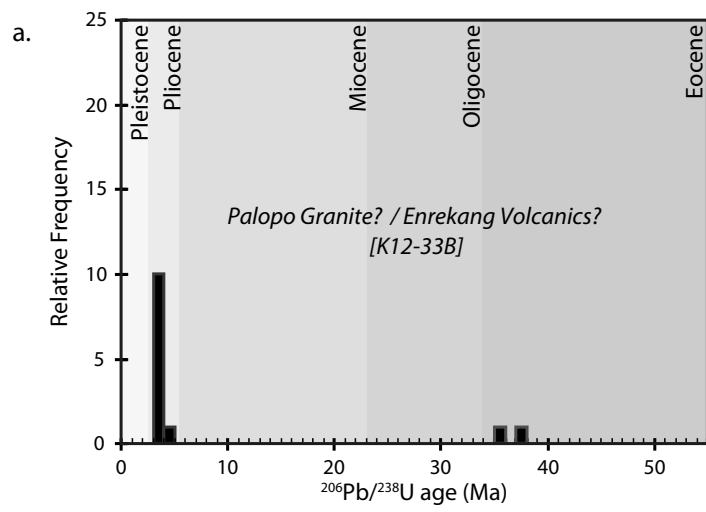


Figure 11

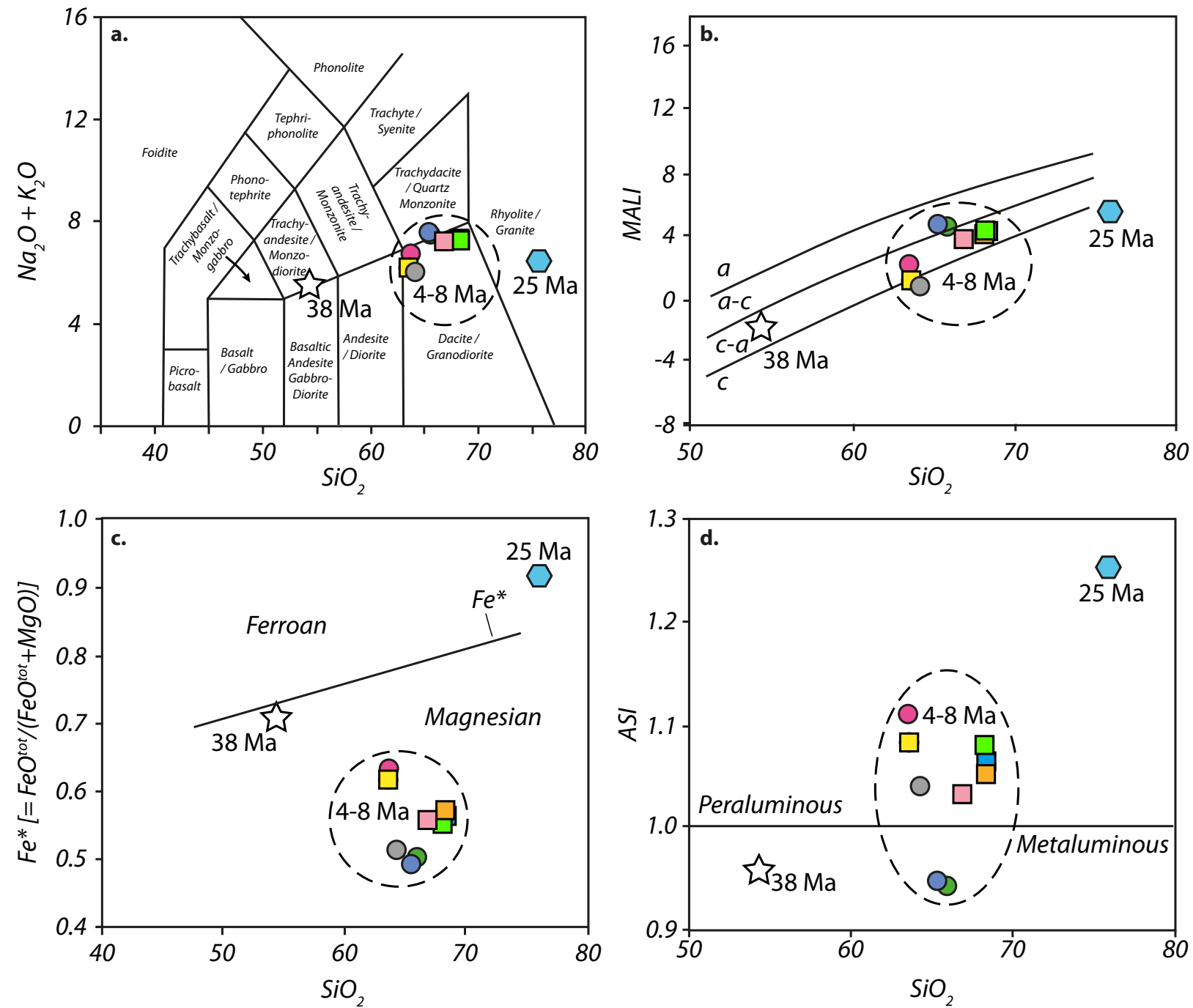


**Figure 12**



**Figure 13**

**Figure 14**



*Enrekang Volcanics*

- K12-33B
- K12-21A
- K12-21B
- K12-27

*Palopo Granite*

- K12-4B
- K12-6A
- K12-6B
- K12-35B
- PA21

*Bua Rhyolite*

- ⬡ K12-31

*Andesite (Lamasi Complex?)*

- ☆ K12-11B

**Figure 15**

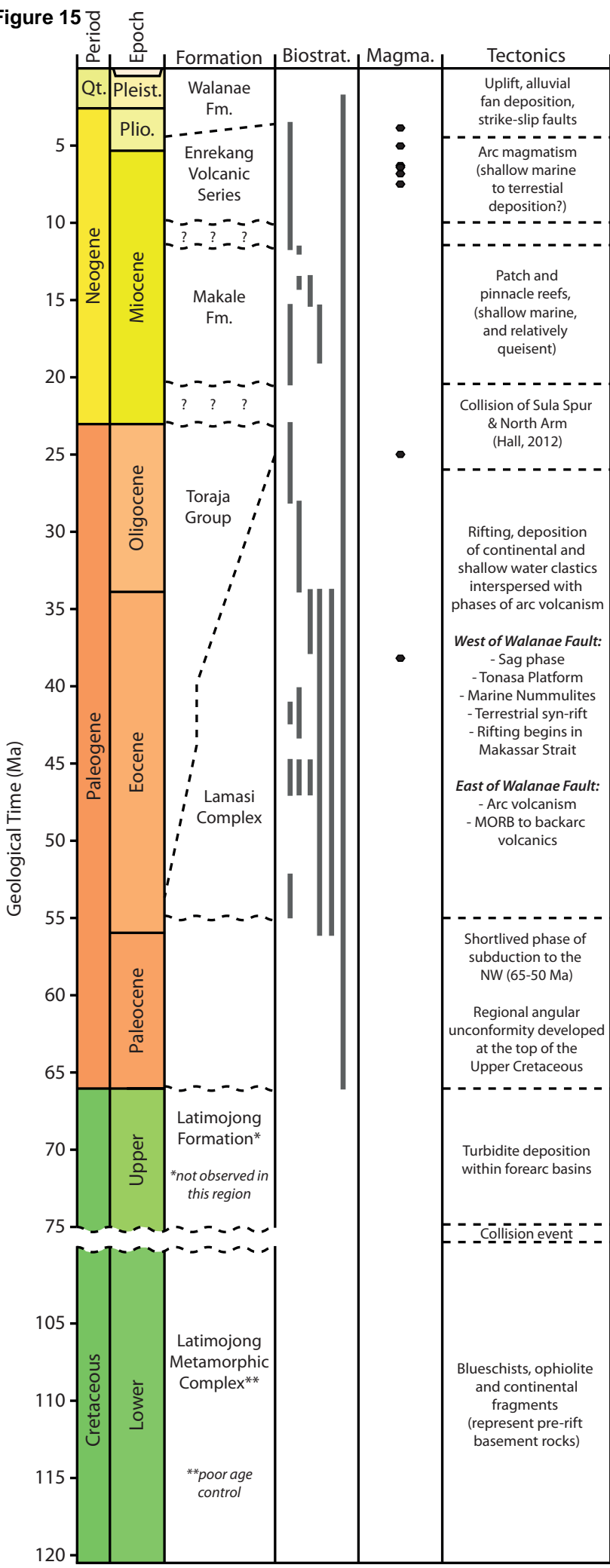


Table 1

Sample	Lat.	Long.	Lithology	Geochem.	U-Pb age ( $\pm 1\sigma$ )
<i>Enrekang Volcanics</i>					
K12-33B	-3.03571	120.11734	Felsic Dyke	x	3.9 Ma $\pm$ 0.1 Ma
K12-21A	-3.51503	119.78141	Dacite (porphyritic)	x	6.8 Ma $\pm$ 0.1 Ma
K12-21B	-3.51503	119.78141	Dacite (porphyritic)	x	-
K12-27	-2.85184	120.10847	Dacite (porphyritic, altered)	x	7.5 Ma $\pm$ 0.1 Ma
<i>Palopo Granite</i>					
K12-4B	-2.95663	120.09621	Granodiorite (undeformed)	x	5.0 Ma $\pm$ 0.1 Ma
K12-35B	-3.02595	120.12712	Granodiorite (deformed)	x	6.3 Ma $\pm$ 0.1 Ma
K12-6A	-2.95646	120.06854	Granodiorite (deformed)	x	-
K12-6B	-2.95646	120.06854	Granodiorite (deformed)	x	6.4 Ma $\pm$ 0.2 Ma
PA21	-2.95253	120.07236	Granodiorite (deformed)	x	-
<i>"Bua Rhyolite"</i>					
K12-31	-3.05184	120.22453	Rhyolite (altered)	x	25.0 Ma $\pm$ 0.7 Ma
<i>Altered Andesite (Lamasi Volcanics?)</i>					
K12-11B	-2.83792	120.02377	Andesite (highly altered)	x	38.2 Ma $\pm$ 1.3 Ma

